



POLITECNICO
MILANO 1863



UNIVERSITAT
POLITÀCNICA
DE VALÈNCIA

DEPARTMENT OF ELECTRONICS, INFORMATION AND
BIOENGINEERING

BACHELOR OF SCIENCE IN BIOMEDICAL ENGINEERING

Development sensorized 3D-printed realistic
phantom to scale for Surgical Training with a
daVinci[®] robot

Author

Pedro Castillo Rosique

Supervisor

Prof. Elena de Momi

Prof. Valery Naranjo

Co-supervisor

Alberto Rota

Contents

Abstract	2
Resumen	3
1. Introduction	4
1.1. Motivation	6
2. State of the Art	
2.1. Introduction to Robotic Assisted Surgery and Da Vinci	8
2.2. Partial Nephrectomy Explanation	11
2.3. Fundamentals of Robotic Surgery Curriculum	14
2.3.1. FRS skills:	
2.3.1.1. Cognitive	15
2.3.1.2. Psychomotor and the dome	16
2.3.1.3. Team training and communications	17
2.4. CT-image segmentation programs and algorithms [2]	18
2.5. Sensorized psychomotor skill assessment platform [3]	23
3. Materials and Methods	
3.1. Segmentation RMI algorithm and 3D modelling	24
3.2. Operation planning belonging to curriculum similarities	37
3.3. Adapting the 3D-model printable, according to FRS requirements	38
3.4. 3D printing	41
3.5. Sensing and data collection	42
3.6. Evaluation metrics	45
3.7. Experimental protocols	47
3.8. Ethical considerations	48
4. Results	50
5. Discussion	57
6. Conclusion	60
Agradecimientos	60
References	61

D.O.G.

Abstract

The increase of surgical procedures using robotic technology in the last decade demands a high number of surgeons capable of teleoperating advanced and complex systems while safely and effectively taking advantage of Robot-Assisted Surgery benefits. Currently, training plans rely on Virtual Reality and simulated environments to achieve a scalable, cost-effective, and comprehensive establishment of robotic surgical skills. This work focuses on the development of a clinical scenario through sensors that assist the surgeon during their training with the daVinci® system, implemented in a 3D-printed physical environment. This research aims to obtain a segmented model, 3D printing the model to simulate the real clinical scenario, thus familiarizing the surgeon with the interaction of organs and tissues with the robot. Additionally, sensors are implemented to assist the surgeon during training. Therefore, to demonstrate the effectiveness of the assistance during the training sessions and the validity of the exercises in the simulated operation, a study was conducted with twelve volunteers. Both visual assistance and the use of 3D phantoms prove to be an optimal alternative for learning the required skills in robotic surgery, representing a significant step forward towards personalized training for each surgeon.

Keywords: RAS, surgical training, segmenting, 3D printing, microcontroller.

Resumen

El aumento de los procedimientos usando la robótica quirúrgica en la última década demanda un alto número de cirujanos, capaces de teleoperar sistemas avanzados y complejos y, al mismo tiempo, de aprovechar los beneficios de la Cirugía Asistida por Robot de forma segura y efectiva. En la actualidad, los planes de formación se basan en la Realidad Virtual y entornos simulados para lograr un establecimiento escalable, rentable y completo del conjunto de habilidades quirúrgicas robóticas. Este trabajo se centra en el desarrollo de un escenario clínico mediante sensores que asistan al cirujano durante su entrenamiento con el *daVinci*[®], implementados en un entorno físico impreso en 3D. Esta investigación busca la obtención de un modelo segmentado, la impresión 3D del modelo para simular el escenario clínico real y así abitar al cirujano a la interacción de los órganos y tejidos con el robot; y la implementación de sensores con que asistir al cirujano en el entrenamiento. Para ello, con el fin de demostrar la eficacia de la asistencia durante los entrenamientos, así como la validez de los ejercicios de la operación simulada se ha realizado un estudio con doce voluntarios. Tanto la asistencia visual como el uso de fantomas 3D muestran ser una alternativa óptima para el aprendizaje de las habilidades requeridas en la cirugía robótica: manifestándose un paso adelante hacia un entrenamiento personalizado para cada cirujano.

Palabras clave: RAS (Cirugía Asistida por Robot), entrenamiento quirúrgico, segmentación, impresión 3D, microcontrolador.

Chapter 1

Introduction

Robotic surgery, since its inception in the 1980s, has brought relevant improvements to the healthcare field by offering safer and more efficient solutions to surgical challenges. Surgical robotics have made their way into various medical specialties, including dentistry, orthopedics, and neurosurgery, as more regulatory organizations increasingly approve novel procedures in these areas. Through the integration of robotic technology, surgeons and medical specialists have been empowered with designed tools to improve their abilities and enhance patient outcomes.

Robot-assisted surgeries embrace the collaboration between medical teams and robotic devices, that are engaged directly with the patient's body. Therefore, there appear to be two distinct approaches to implementing robotic assistance in the operating rooms: teleoperated systems and image-guided systems [1].

Teleoperated systems appeals the user, who directly and continuously interacts with the robot, controlling the robot's movements primarily through hand-held manipulators that replicate the surgeon's own motions. Whereas, image-guided systems rely on medical imaging data, such as CT scans or MRIs, to plan the robotic tools movements and incision tryectory, not being, hence, a direct and real-time interface between the surgeon and the robot, but a previous assistance.

In such sense, the new paradigm of the Human-Robotic Interaction [2] arises from the approach that surgical robots augment the capabilities of the surgeons, relaying on them the final control of the devices, for which both *robot-assisted* techniques can be implemented together, offering the surgeon an aid before and after the surgical procedure.

An example of surgical robotic system is the daVinci® (Intuitive Surgical, Inc.), which is one of the first surgical robot to get the approval from different regulatory affair agencies. This surgical devices are extremely complex, and thus, request a long and intensive training to comply optimal performances and ensure patients safety. In this sense, at the early stage of the trainings, semi-realistic plastic phantoms, and either animals and cadevers were used, but over the years, the development of virtual reality, Deep Learning and AI-based computer vision techniques have opened a new paradigm in the trianing approach, simulating surgical scenarios with a certain level of realism, where the interaction between the virtual elements is emulated by the software, considering ecuations that approximate reality.

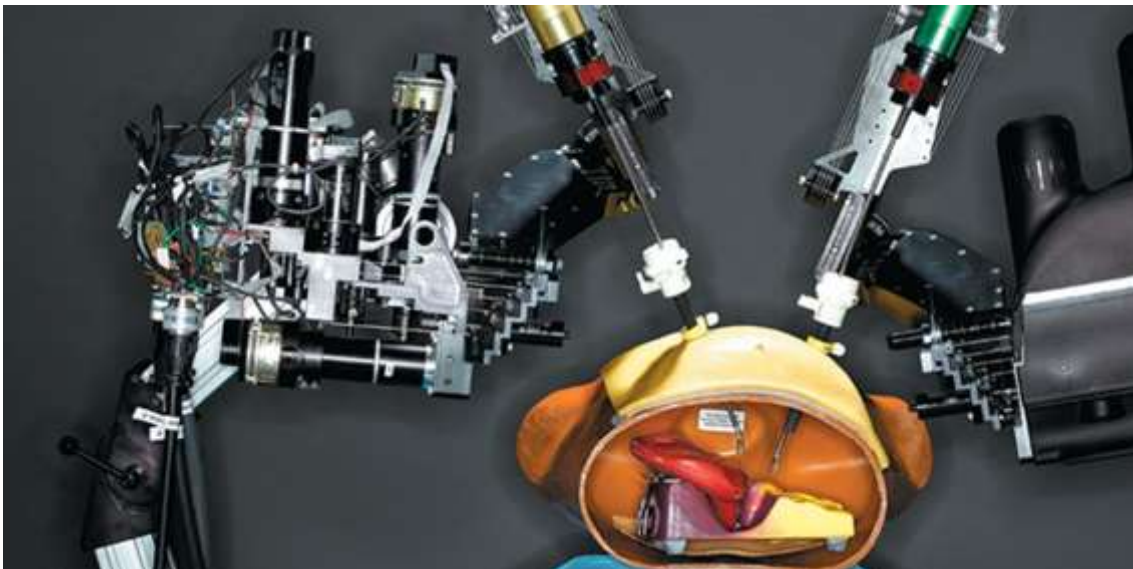


Figure 1. 1: A phantom model. Photo courtesy of IEEE Xplore.

Surgical assistance emerges as a significant factor in surgical robotic trainings as an efficient, objective and semi-autonomous approach to new training styles, as there would not be a person glancing the trainee constantly. An example of this are visual cues, that may warn the surgeon whenever some sensitive structures are touched or, for instance, could help in the procedure guidance.

In fact, the aim of this work is the development of a plastical realistic phantom with diverse impemented sensors, focusing on assessing the trainees through visual cues and collecting data.

1.1. Motivation

Surgical robotics training is the first step in the manipulation of the surgical robots, aiming to achieve the skill transfer of high specific set, including cognitive, psychomotor and communication with the clinical staff in the Operatory Room. [3]



Figure 1. 2: A surgeon using a daVinci® robot. Photo courtesy of *Intuitive Surgical Inc.*

In the past, training programs in surgical robotics were only given for experienced surgeons with prior background in laparoscopic surgery, because of the limited number of devices available. Over the years, this has been extended to medical students and residents, who deepen into this field as a specialization medical educational program. In addition, the rejection and distrust towards surgical robots in operating rooms made it necessary to prove their efficiency scientifically, by comparasing the enhanced outputs when appealing surgical devices [4].

Whitin this scope of developing assesed training and the study of the benefits of robotic surgery , appears the chance of implementing sensors for assessing trainees during the training, guaranteeing the development of their necessary skillsets.

The development of virtual reality, also, has fostered the development of simulated scenarios used for skill acquisition, nonetheless it needs to replicating reality and computational cost. For this reason, the aim of this work is the design of a sensorized phantom in which realism and sensing are the main objectives and the hypothesis stated is to prove the utility of using a plastic realistic phantom with sensors embedded for assessing robotic surgical training.

Chapter 2

State of the Art

2.1. The daVinci® Surgical System Surgery

For the last decades, technological development in the medical field and the willingness to lower the impact of surgeries on patients promoted the invention of laparoscopic surgery dating back to 1901, when it was practised on an animal, but not until the 1980s that was in humans [5]. This technique consists of accessing the abdomen and pelvis without having to make large incisions in the skin, resulting in fewer postoperative days at the hospital, and pain as the tissue stress is lower than in traditional surgeries. Not only but also the physical anatomical results are better, and even the recovery from the whole operation is shorter. [6]

Parararily, the implementation of telemonitoring and computer-aided instruments in surgical proceedings has come to what is known as robotic-operation-systems (ROS), which is defined as: “Medical Electrical Equipment/System that incorporates programmable electrical medical system actuated mechanism intended to facilitate the placement or manipulation of Robotic Surgical Instrument”[7]. Nevertheless, before the appearance of ROS, early robot prototypes, developed by Computer Motion Co., for instance, focused on endoscopic camera holders named AESOP (Automated Endoscopic System for Optimal Positioning), used as camera assistance. Over time, this robot was extended, making it capable of carrying a wide range of surgical instruments with the name of Zeus.

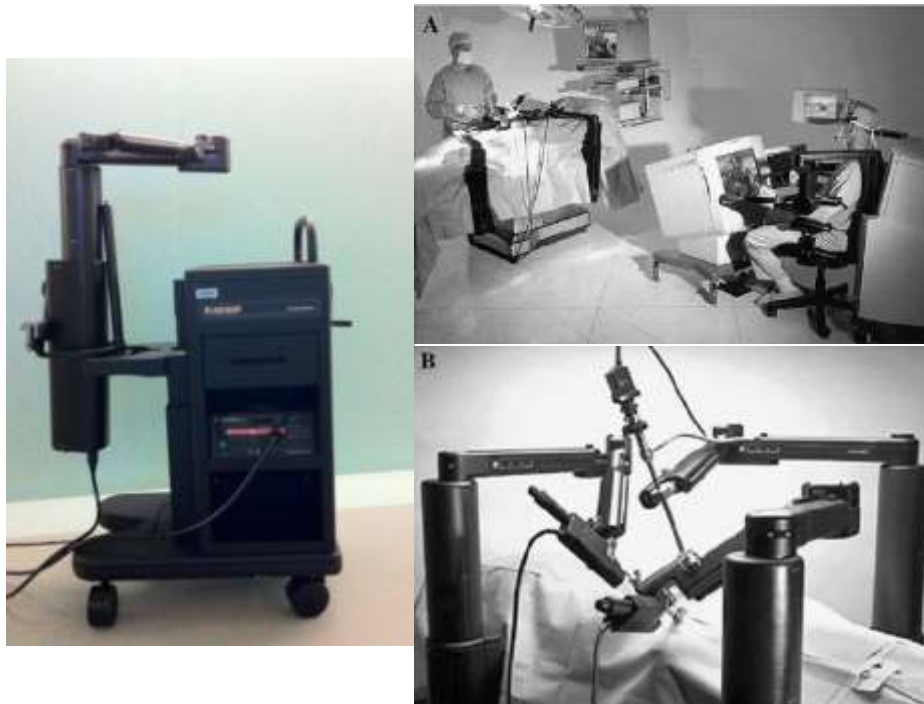


Figure 2. 1: Different photos of the first surgical robotic devices.

At the beginning of medical robotics, dexterity and impaired view control were the main problems to enhance after the first ROS proceedings. So, primary attempts at robotic surgery were related to camera guidance systems, willing that surgeons were somehow coordinated with the ROS, helping in the vision of the patient's anatomy, and getting better images of the scene. As an example, in 1998 the British company Armstrong Healthcare developed a camera robot that moved synchronously with the surgeon's head, solving one of these problems.

Whilst optimizing dexterity, the concept of master-slave was developed as a bridge between the surgeon's movements and the end effectors of the instruments used, in the sense that, while an operator made some gestures, the device translated those manoeuvres into the surgical instrumentation. In fact, this concept was originally developed by the National Aeronautics and Space Administration (NASA) [8], to enable telesurgery, with the idea of providing medical assistance to astronauts in space, remotely. Later on, the Defense Advanced Research Projects Agency (DARPA) also invested many resources in researching on telesurgery, wondering also about teleoperating soldiers in perilous situations such as battlefields or people carrying

infectious diseases. The Green telepresence system was carried out by them and intended to be a prototype for teleoperation; but in terms of structure and functionality is considered the predecessor of the daVinci® surgical robot because it was provided with all the requirements that were been researched. [9]. With that, da Vinci and Zeus were the first teleoperated minimally invasive surgery systems launched into the market by the end of the 20th century.



Figure 2. 2: A surgeon using the first daVinci® surgical robot.

Actually, medical robots are used not only for surgery, but also acquiring pre-operative images for planification or real-time monitoring of the procedure, obtaining quantitative information (e.g. the active sides of a brain during a fMRI), including methods for image processing, spatial comprehension and planning [10]. These new features make it easier for surgeons, as they have previous valuable information, and ROS allows them to use their traditional skillsets while operating. Otherwise, basic manoeuvres, such as suturing, proceeded laparoscopically, would require highly technical skills. Another consideration is, the convenience for doctors compared to traditional laparoscopy; instead of staring at a screen while operating and, with that, losing hand-eye coordination and accuracy, they are positioned comfortably reducing cognitive dullness. [6]

To continue, the daVinci is composed of three different subsystems: the patient side cart, the surgeon console, and the vision cart. It relies on four key specifications, similar to the two requirements described upper: first, the system has to be reliable and failsafe, in case there was any error, to preserve the feasibility during the procedure; secondly, the system needs to provide intuitive control of the ROS resembling natural operating movements, as in traditional surgery. The third purpose is for the ROS to have six degrees-of-freedom and a functional gripper, enhancing the procedure of common laparoscopy. The fourth pillar is being able to get a 3D image of the patient's anatomy willing to increase the perception during the operation, as haptics are lost. [11]

2.2. Partial Nephrectomy Explanation

Partial nephrectomy is a clinical procedure considered the standard gold treatment of clinical T1 renal masses that, during the years, has spread with the development of minimally invasive techniques such as laparoscopy and ROS.

Focusing on the procedure performed by ROSs, its 3D magnification and stereoscopic vision, followed by the degrees of freedom of the PSM's, justifies the diffusion of these techniques over the rest, as it also has a shorter learning curve and can easily implement other types of new technologies, for instance, image guided systems. [12]

Indications about when to perform the procedure, consider mainly T1 kidney tumors preceded with either open, traditional laparoscopy or ROS. However, one of the features to consider when deciding the technic is the surgical complexity and the large size of the tumor, which are factors that are still under scrutiny when considering robotic approaches. Therefore, it stills in clinical trial the procedure for T3a tumor stages.

According to the technique to perform the surgical act, some guidelines have been standardised; nevertheless, the approach to the surgery is often left to the decision of the surgeon and his convenience. Nonetheless, regardless of the surgeon, some general steps can be conducted: [13]

Step 1: starts with the insufflation and the docking of the surgical equipment in either a transperitoneal or retroperitoneal approach, *figure 2.3*. The first one has the advantage of a larger working space and more familiar anatomical landmarks for guiding the surgeon, whilst retroperitoneal allows for avoiding the peritoneum's incision and the opening of the abdominal cavity. The instruments introduced for the Si System version of the da Vinci robot consists of three trocars and cannulae that correspond to what is known as Patient Side Manipulator (PSM) and two 12 mm disposable trocars where the camera, the assistant and an insufflation needle are placed.

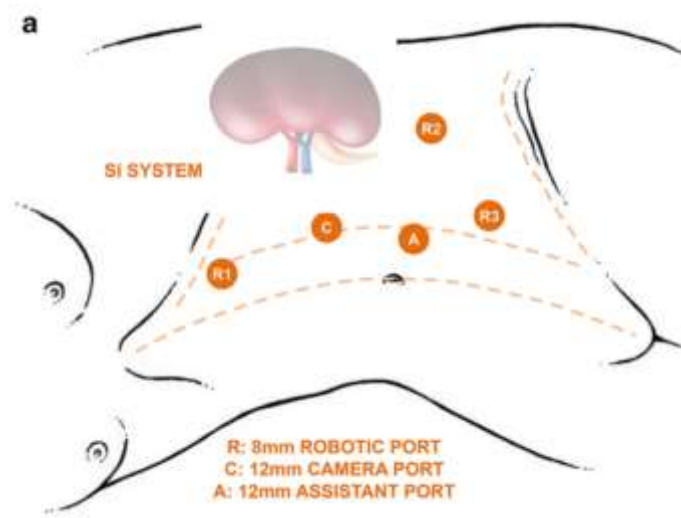


Figure 2. 3: Placement of the surgical tools in a partial nephrectomy. Photo courtesy of SpringerLink.

Step 2 consists of the reflection of the colon, as it exposes the kidney once the peritoneum and Gerota's fascia are visible along the medial length of the kidney. In this situation, the surgeon may see that the perinephric fat and Gerota's fascia often appear more yellow than the mesenteric fat. Continuing, the mesenteric fat and the colo-renal attachments can be retracted by the assistant or the fourth arm. The anatomical structures found on the right are the ureter and the vena cava; and on the left, the resting ureter and the gonadal vein. Some warnings during this procedure are, to stay away from the iliac vessels and the appendix when incising the peritoneum near the pelvis, and when dissecting the colon not to hit the duodenum and the pancreas.

The lateral retraction of the kidney, **step 3**, is done in order to free the renal hilum and stretch it after suspending the kidney. As such, within the renal hilum, more working

space appears between the kidney and the great vessels. Therefore, this movement exposes the remaining colo-renal attachments and can be easily removed. Moreover, the next step is to identify the gonadal vein to the cava and trace the renal vein.

The **4th step** consists of dissecting the adrenal gland from the upper pole of the kidney, especially for tumours in the above part of the kidney, not mandatory in lower neither midpole tumours... The adrenal gland is recognised easily for its yellow appearance, and is removed by using the dual-blade retractor linked to the fourth arm, using monopolar scissors and prograsp instruments throughout the resting arms.

Hence, the surgeon will be cutting along the lateral border of the aorta, on the left side, suggesting awareness during this step. Moreover, the surgeon may incise the lateral splenic attachments close to the diaphragm, causing the partial dislodgement of the spleen, obtaining the desired exposure.

The **fifth step** intends to remove the fat around the lesion, exposing the renal parenchyma. For this task, the instrument list does not change with respect to the other step, but includes using a laparoscopic ultrasound probe to identify the tumour. Showing the parenchyma is relatively easy except in patients with abundant adherent fat, expecting to avoid these types of patients in their initial experience, as later, the parenchyma is sewn for closing the wound. Moreover, intraoperative ultrasound defines the edges of the resection and provides the surgeon a mental image of the margins of the tumour.

6th step looks for clamping the renal hilum. For this, different types of bulldogs are used to occlude the vascular irrigation to the kidney, and therefore, the carcinoma, having administrated mannitol and furosemide before the procedure. The hilum, before the occlusion has to be exposed by lifting the lower pole of the kidney, to clamp the renal artery but not the cava vein, which is optional. After the occlusion, the stopwatch should start so that the surgeon is aware of the cumulative clamp time, which the anesthesiologist will announce every ten minutes.

Step seven is for the tumour excision aiming to achieve a negative edge in the histology study of the carcinoma, for which different image tools can be applied to identify the lesion easily. After the excision, the surgeon circulates frozen pieces of the tumour to be

analysed; however, the reconstruction has already started by the time the results are delivered. During the removal of the tumour, bleeding and oozing are common at the beginning; nonetheless, remaining, after some minutes, would express previous uncompleted steps.

Reconstruction of the wound is the **eighth step**, for which is only used a needle driver with an oversewn through a thread 2-0 vicryl suture on an SH needle. The suture may be tied, and some clips used to secure the procedure. Furthermore, larger veins or arteries can be sutured with figure-of-eight not and the parenchyma closed every centimetre with a #1 vicryl suture on a CT needle. The stitches are sewn every seven centimetres, also passing the suture through the parenchyma.

After sewing different stitches, the vein and the artery are unclamped; however, if some bleeding is sighted, more stitches should have to be placed. Alternatively, some surgeons use thrombogenic material to fill the renal defect. After the surgeon's satisfaction of the procedure, the vessels are unclamped.

Finally, the placement of the drain is placed to extract the resting liquids and oozing wound. Also, the PSMs are undocked, the surgeon scrubs the overall scenario and the specimen is entrapped into a sack and extracted from the body. Finishing the procedure by introducing the drain within a new puncture.

2.3. Fundamentals in Robotic Surgery

Once the partial nephrectomy has been shown, it is important to determine which abilities surgeons must have to ensure proper procedure and guarantee a comprehension of the basics of robotic surgery, regardless of their speciality. Within the background of the Fundamentals of Laparoscopic Surgery (FLS) curriculum, the Department of Defense, Veterans Administration and fourteen surgical speciality societies wrote the Fundamentals of Robotic Surgery (FRS) curriculum; which are two assessment tools: a curriculum for knowledge and team training skills and a device for psychomotor skill training and evaluation, that are based on a set of 25 robotic surgery concepts previously determined table 2.1. [14]

This FRS curriculum is required to guarantee proper performance of any ROS and a clear comprehension of the basis of communication skills during any procedure; assuming that pre-operative care and post-operative care are already known by the surgeon. The final result of the congress, therefore, was a curriculum that compasses the cognitive, psychomotor and team training skills.

<i>Pre-operative</i>	<i>Intra-operative</i>	<i>Post-operative</i>
System settings	Energy sources	Transition to bedside assistant
Ergonomic positioning	Camera control	Undocking
Docking	Clutching	
Robotic trocars	Instrument exchange	
Operating room set-up	Foreign body management	
Situation awareness	Multi-arm control	
Closed-loop communications	Eye-hand instrument coordination	
Response to system errors	Wrist articulation	
	Atraumatic tissue handling	
	Dissection-fine and blunt cutting	
	Needle driving	
	Suture handling	
	Knot tying	
	Safety of operative field	

Table 2.1: list of the FRS curriculum.

Cognitive skills: The didactic and knowledge part outlines the didactic material that should be taught to the surgeons. The content includes a description of each of the main ideas shown in the outline, with a list of errors and solutions that a trainee should get familiar with. Moreover, this material is delivered in several formats (i.e. lectures, slide presentations, multimedia content, etc).

The major ideas of this section are: 1. An introduction to the principles and functionality of robotic surgical devices. 2. Pre-operative set-up of equipment and positioning of the patient and staff, placement of the passive joints, checklist and commissioning. 3. Intra-operative use of the robot, description of the limitations of the psychomotor skills, operative control of the robot and necessary instruments and supplies. Furthermore, the communication skills of the surgeon with the staff. 4. Post-operative steps according to shutting down the robot and removing it from above the patient.

In the introduction to surgical devices, an overview of the principles of robotic surgery is made, also as a contrast with laparoscopy; continued by an explanation of the surgical components, leaving space for further inventions. The second part talks about the

preparation of the robot and the staff. The intra-operative section is related to how to do a proper operation providing a list of errors that may appear, focusing on ensuring the patient's safety. Finally, the post-operative phase explains how to remove the device correctly.

Psychomotor skills: This section refers to any performance that draws on, a combined and coordinated set of a cognitive and motor processes. For this, the group selected seven principles for further deciding which skills surgeons need.

These principles are: 1) The tasks should be three-dimensional in nature. 2) The tasks designed for learning, should include multiple skills at once. 3) The skills should be designed to train the full capability of the robotic system. To include skills and tasks that are not possible in open or laparoscopic surgery. 4) Implementation of the tasks and the resultant method for teaching should not be cost-prohibitive. 5) High-fidelity models should be used for testing. Training can use lower-fidelity devices and methods. 6) Tasks should be easy to administer, to ensure inter-rater reliability. 7) The tasks should be designed for implementation with physical objects and devices. The device will be developed initially in virtual reality as a CAD/CAM model, from which the actual physical models will be 'printed', creating a training experience that would be identical in both the virtual and real world.

After doing that, they defined 16 main capacities, from the 25 skills table, referring to the psychomotor skills, conditions, metrics and errors more common in each situation. Ten of them were mainly created for the learning device, and the others were selected from the FLS or existing educational programmes. All this also led to the development of the 'FRS dome', conceived to be the device where all these tasks were put into practice, which will be explained later.

According to the abovementioned principles, the committee developed a device, called the 'FRS dome', to practice the 16 abilities. Also, they summarised these capabilities in seven exercises related to the dome. These are: 1) *Docking and instrument insertion*. 2) *Ring Tower transfer*. 3) *Knot tying*. 4) *Railroad track*. 5) *4th arm cutting*. 6) *Puzzle piece*. 7) *Vessel energy dissection*. Taking a look at the table 2.2.





<p>Task 1: Docking & Instrument Insertion:</p> 	<ul style="list-style-type: none"> - Docking - Instrument insertion - Eye-hand coordination - Operative field of view
<p>Task 2: Ring Tower Transfer:</p> 	<ul style="list-style-type: none"> - Eye-hand coordination - Camera navigation - Clutching - Wrist articulation - A-traumatic handling
<p>Task 3: Knot Tying:</p> 	<ul style="list-style-type: none"> - Knot tying - Suture handling - Eye-hand coordination - Wrist articulation
<p>Task 4: Railroad Track:</p> 	<ul style="list-style-type: none"> - Needle handling & manipulation - Wrist articulation - A-traumatic handling - Eye-hand coordination

Table 2.2: description of the basic psychomotor skills attached to the seven FRS tasks.

Therefore, when a dome is being designed, these tasks must be considered to preserve the minimal assessment standard for ROS.

Team and training communications: They started by explaining the importance of team training and concrete communication, among the robotic surgical procedures, as a key component for successful team building. Which came into some main ideas: 1) Team alignment with common objectives. 2) Inclusion. 3) Empowerment of all the staff. 4) Shared ownership and responsibility. 5) Person-specific directives. 6) Task management and completion. 7) Reiterative or ‘Just in time’, performing all the tasks coordinately and efficiently. 8) Going from risk management to quality improvement through a closed loop.

This part of the curriculum was written following the scheme of other existing programmes to where it was extrapolated. The document is composed of a checklist whose points are: 1) *Pre-operative*: related to addressing the general situation, elements and functions of the surgery room. 2) *Robotic Docking Checklist*. 3) *Intra-operative*:

communicating with staff during the operation, taking into consideration that once the operation begins, surgeons do not have visual contact with the operating team. 4) *Undocking & post-operative.* 5) *Debriefing.*

Furthermore, a list of communication behaviours was also described emphasising those critical situations in which team building is most important. Some of them are: 1) Instrument exchange steps. 2) Specimen management. 3) Foreign body management. 4) Retiring hands from the operating area. 5) Checking intraoperative list. 6) Recognition and management of perilous situations.

Finally, the curriculum was bound to be taught, using test questions, video clips and simulators with situations such as urgent undocking of the ROS, team empowerment... [15] [16].

2.4. Segmentation tools and CT-image segmentation programs.

Apart from the main scope of the Thesis, which is the design of a dome, segmentation processes are used for surgical planning in complex surgical situations where providing the surgeon with a printed-specific 3D model or an augmented reality sample. This is widely applied to oncological surgical planning providing a better understanding of the spatial relations between the tumour and the organs around it. Pre-aperture model usage is getting increasingly important in today's operation schedule as they gather much relevant information, helping doctors guide the procedure. [17]

Segmentation techniques

This section of the work focuses on the research of previous CT-images segmentation programs. Considering that depending on the modality of the image and the organs targeted it would be chosen one or other program but, as the aim of the research is to get a complete womb 3D model, it is only possible to get an embracing model for a few organs rather than a general algorithm.

According to the segmentation tools, there exist many different techniques to segment an image considering the brightness of the voxel or the geometrical position, founding

a set of algorithms: thresholds, growing seed regions, watersheds, clustering (K-means, Fuzzy c-means, hierarchical models, mean shift), neuronal networks, technics based on probabilistic atlas (Expectation maximisation) and multi-atlas. h

As described in *table 2.3* of the Paper: ‘ Comprehensive Review of 3D Segmentation Software Tools for MRI Usable for Pelvic Surgery Planning’, there is a wide list of segmentation programs available on Internet considering some variables such as automatic segmentation, usability, segmentation time and the cost.

It is important to remember that there was no previous knowledge in this field, and therefore, there has been a learning process along the way. Also, because the pre-aperture model englobes many organs, the features of the program had to be as general as possible.

Software	Automatization	Usability	3D visualization	Segmentation time	Registration	Tractography	OS		
							Windows	Linux	Macintosh
3D Slicer	3	3	4	15th	x	x	x	x	x
Anatomist	1	1	1	>25 h			x	x	x
AW Server	3	3	3	>20 h	x	x	x		x
Freesurfer	2	2	1	>20 h	x	x		x	x
FSL	1	1	2	>25 h	x	x		x	x
ImageJ	2	2	1	>25 h	x		x	x	x
ITK-SNAP	3	4	4	10 h			x	x	x
Mango	1	3	2	>20 h	x		x	x	x
MedInria	3	3	3	>20 h	x	x	x	x	x
MIPAV	3	2	2	>20 h	x	x	x	x	x
Myrian Studio	3	3	4	9 h	x		x		
Olea Sphere	3	33	4	>20 h	x	x	x	x	x
OsiriX	3	3	4	>20 h	x				x
Seg3D	2	4	3	20 h			x	x	x

Table 2.3: description of the programs commonly used for semgention.

It could have been possible to make a comparison model in order to evaluate the segmentation done, but since it is a new model, it has yet to be possible to find a ground truth.

Going further on the explanation of the software used, some considerations about the tools for segmenting will also be explained. Segmenting consists of assigning the part of the image that corresponds to the anatomical that represents. Some tools exist for doing these tasks based on different properties of the image, as for example, brightness, color, etc. [18]

In this sense, threshold tools, put into a binary value those pixels in the image which have an upper, lower or interval level of intensity, giving them a corresponding label that is linked with, in biomedical image cases, with anatomical parts of the body. The cases that could be studied are:

$$I(x) = \begin{cases} 0 & x \leq th \\ 1 & x > th \end{cases}$$

$$I(x) = \begin{cases} 1 & \text{if } lower_thd < x < \\ & upper_thd \end{cases}$$

$$I(x) = \begin{cases} 1 & \text{if } x \geq threshold \\ 0 & \text{if } x < threshold \end{cases}$$

Being x the value that determines the pixel of each image and the value returned the value according to each pixel.

It can be understood by seeing an image's histogram, as shown in figure 2.4. The threshold would be determining a limit in the intensity axis and selecting a group of pixels.

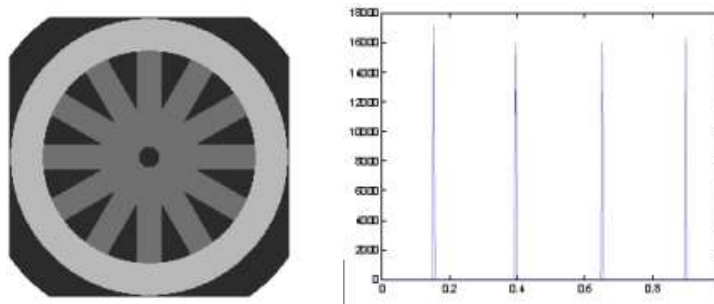


Figure 2. 4: Example of an histogram.

Another common tool used for image segmentation is the region-growing seeds. This works by applying a pixel as a seed that belongs to a certain region depending on the criteria. The connectivity can be to 4 or 8, which means comparing the neighbour pixels

surrounding the seed. The criteria to be applied is known as region homogeneity, which compares the intensity value of the neighbour with the seed process called Connected threshold. The other parameter that could be considered is Confidence connectivity, which is based on including or not the neighbour pixels if their intensity is between two intervals.

$$f(x) = \begin{cases} 1 & \text{if } [m(x) - ts, m(x) + ts] \\ 0 & \text{if rest} \end{cases}$$

Being the m the mean of the region, s the typical deviation and t the tolerance, which is the parameter that will be modified intending to be more or less conservative with the pixel selection. By this, the mean and deviation parameters upload each time a pixel is added.

Another image processing tool specially used in medical imaging is mask processing which refers to a binary or grayscale image that is used to modify or analyze specific regions of an input image selectively. It acts as a filtering mechanism, allowing certain portions of the image to be preserved or altered while disregarding the rest. Typically, a mask consists of pixel values that correspond to the degree of transparency or importance assigned to each pixel in the original image. They provide a powerful means to isolate and manipulate regions of interest, facilitating precise control and manipulation of visual data in diverse applications. As seen in figure 2.5. [19]



Figure 2. 5: Example of the algorithm growing from seeds.

Finally, in image processing but also in volume rendering, smoothing factors are also used to make segment boundaries softer by removing extrusion and filling small holes. These factors can be split in:

Median: The median filter operates by replacing each pixel in the image with the median value of its neighbouring pixels. Unlike other filters that use mathematical averaging, the median filter is particularly effective at removing impulse or "salt-and-pepper" noise, which appears as randomly isolated pixels with extreme intensity values. The filter disregards outliers by taking the median value, resulting in smoother images while preserving the important edges and details.

Gaussian: works by convolving the image with a Gaussian kernel, which is a bell-shaped function that assigns weigh

ts to neighboring pixels based on their proximity to the center pixel. The Gaussian filter is advantageous because it preserves edges and fine details while reducing noise and unwanted high-frequency components. By applying a Gaussian blur, image imperfections are smoothed out, resulting in a more visually pleasing and less noisy image.

Opening: Opening is another morphological operation in image processing that involves the sequential application of erosion followed by dilation. It is primarily used for removing small bright regions or white noise while preserving the larger-scale structures in an image. The process starts with an erosion operation, which erodes away the boundaries of objects and removes small protrusions. This is followed by a dilation operation, which expands the eroded objects, bringing them closer to their original size while still eliminating smaller components.

Closing: Closing is a morphological operation in image processing that combines dilation and erosion to effectively close gaps and fill holes in objects within an image. It is primarily used for removing small dark regions or black noise while preserving objects' overall shape and structure. The process involves applying a dilation operation to expand the boundaries of objects, followed by an erosion operation to shrink the boundaries back. The combination of these operations helps to bridge gaps and smooth out irregularities in the image.

2.5 Sensorized psychomotor skill assessment platform

The last part of the state of the art, consists of a further analysis of what has been previously done in the design of realistic psychomotor skill assessment platforms in surgical scenarios. [6] [20]

In the topic of Robotic Assisted Minimally Invasive Surgery (RAMIS), the spread of its use as an alternative to virtual platforms, increased the importance of data collection tools for having personalised guidance and result assessment after the procedure. In this sense, it fostered the elaboration of data collection algorithms and made these processes simpler since kinematic and kinetic data can be obtained directly from the main robot. In order to get the most objective skill evaluation, the data on which the assessment could be based on are those provided by the robot. In this sense, most of the research conducted consists of collecting internal data from kinematic of the surgical robot, as is information for which no more extensions or hardware implementations are required.

Most of the research conducted on RAMIS related to physical evaluating scenarios, has used the dome that follows the FRS and is generally used after virtual training. Mostly implemented on, the FRS dome different technologies from where to get the data, store the data and conclude with some feedback from the simulated procedure. These evaluations start with deciding the surgical tasks pointed to be assisted and study on which way it could be measured, therefore providing an objective data collection. Based on that information, it could be given an objective assessment of how the training tasks

have been performed. As an example of how the FRS tasks could be studied, this table has been raised from [19].

FRS task	Docking	Ring Transfer	Knot Tying	Suturing	4 th Arm Cutting	Puzzle Piece Dissection	Vessel Dissection
Description	Docking & Instrument insertion	Transfer the ring from one S-shaped tower onto the other	Tie a knot to approximate the eyelets of the I-shaped towers	Horizontal mattress suturing through the target points	Hold and cut the band using the 4 th arms	Cut the puzzle piece pattern staying inside the line	Dissect, seal and cut the vessel
Important factors	All devices and the entire dome should be in the field of view	Wire-instrument collisions, breaking the ring or wires	Appropriate knot, tower-movements	Wound approximation, accurate targeting, tissue-tearing	Accurate cutting, appropriate tension, dropping the vein	Accurate cutting, Tissue handling	Accuracy, blood loss, injury of the vessel
Measured metrics	None	<ul style="list-style-type: none"> - Time - Forces - Contact time - Tower movement - Tower falls 	<ul style="list-style-type: none"> - Time - Forces - Tower movement - Tower falls - Eyelets touching 	<ul style="list-style-type: none"> - Time - Forces - Wound approximation at 4 points 	<ul style="list-style-type: none"> - Time - Accuracy of cutting on the 3 marks (manual evaluation) 	<ul style="list-style-type: none"> - Time - Forces - Accuracy of cutting inside the line (percentage of total cut-length) 	<ul style="list-style-type: none"> - Time - Forces - Vessel- injury (manual evaluation) - Proper cut
Sensors and methods	None	<ul style="list-style-type: none"> - Load cells - Capacitive proximity sensor - Hall-sensor 	<ul style="list-style-type: none"> - Load cells - Capacitive proximity sensor - Hall-sensors 	<ul style="list-style-type: none"> - Load cells - Touch sensors 	<ul style="list-style-type: none"> - Self evaluation via Graphical User Interface (GUI) 	<ul style="list-style-type: none"> - Load cells - Image processing 	<ul style="list-style-type: none"> - Load cells - Continuity-sensor

Table 2.4: description of the variables and its relation to the sensors used in [19].

Chapter 3

Materials and Methods:

In this section, the tools and the process developed during the tasks, hence, 3D-slicer, UltimateMaker 3D-printer, Microcontroller and sensors, and the daVinci Research Kit (dVRK) robotic platform, will be explained. Moreover, the methodology of the data to be collected and how to store it in the computer. Finally, the experimental side will be described, explaining the simulated procedure and which metrics will be conducted.

3.1 Segmentation RMI algorithm and 3D modelling.

3D-Slicer is a powerful open-source software used for medical image analysis and visualisation. It enables the creation of three-dimensional models from medical image data such as CT or MRI scans. Its wide range of tools and modules allows researchers and clinicians to perform advanced image processing, segmentation, and image-guided interventions. Playing an important role in aiding medical professionals in understanding and diagnosing complex anatomical structures and diseases.

For its use, 3D-Slicer version 5.2.2 was installed, including some package tools, called `SegmentEditorExtraEffects` and `SlicerDevelopmentToolbox`, providing further techniques to segment. The overall program offers a wide set of manual tools that could be classified depending on the spatial, quantitative or geometrical features extracted from the voxel.

According to the intensity tools, there is the threshold algorithm and the smoothing factors: Gaussian and Median; which are the most used. Moreover, the quantitative measures the number of voxels that compose the segment. Based on that information, the method Islands, enables to split or join different segments. Another complement that uses the geometrical space is the opening and closing morphological operators, to which the size of the structural element can be chosen, but not its shape. Regarding, morphological tools, but not included in the geometrical group, there are also the subtract and intersect tools between the segments. Finally, Grow from Seeds which is

an automated method that works for various structures and imaging modalities and implements the GrowCut method as Clustering, works by passing the algorithm two masks in a enough number of slides so that the method gets to identify the organ's edges, one that marks the edges of the outer part of the organ and another that corresponds to the infill of the organ. Finally, the scissors, erase, and painting tools depend only on the interpretation of the clinician; but could be used for more trivial modifications.

Image display is also an important factor when segmenting, allowing the clinician to interpret each of the segments of the organs that have been captured within the medical image. 3D-Slicer allows transforming the intensity of the pixels by using thresholds, increasing sharpness between anatomical structures. Filter implementation on the slides, is also another efficacious tool when the quality of the image disturbs boundaries interpretation.



Figure 3.1: display of the frontal view from the patient's file.

The aim of this part was to get a complete segment process drawn up from an anonymous DICOM file of the dicomlibrary.com funded by a European project, in which the patient had to overcome a partial nephrectomy operation. The CT file is composed of 361 slides, showing from the T12 to the First Sacral of the spinal cord.

For both first segments, a B/W level from 100W-70L has been used, getting the display shown in Figure 3.1, enhancing the contrast of the right kidney and the arterial blood vessels.

The **right kidney** was obtained using a Threshold intensity selection between a range of [150-220], getting to figure 3.2. The noise is corrected by using the scissors, and moreover, in order to fill the holes from the surface, because of the threshold, an opening with a structural element of 7x7x7 pixels was done, also some small groups of pixels were removed by the tool Islands. Finally, using Painting, the kidney's surface was filled and smoothed by a Gaussian $\sigma=1,1$ mm.

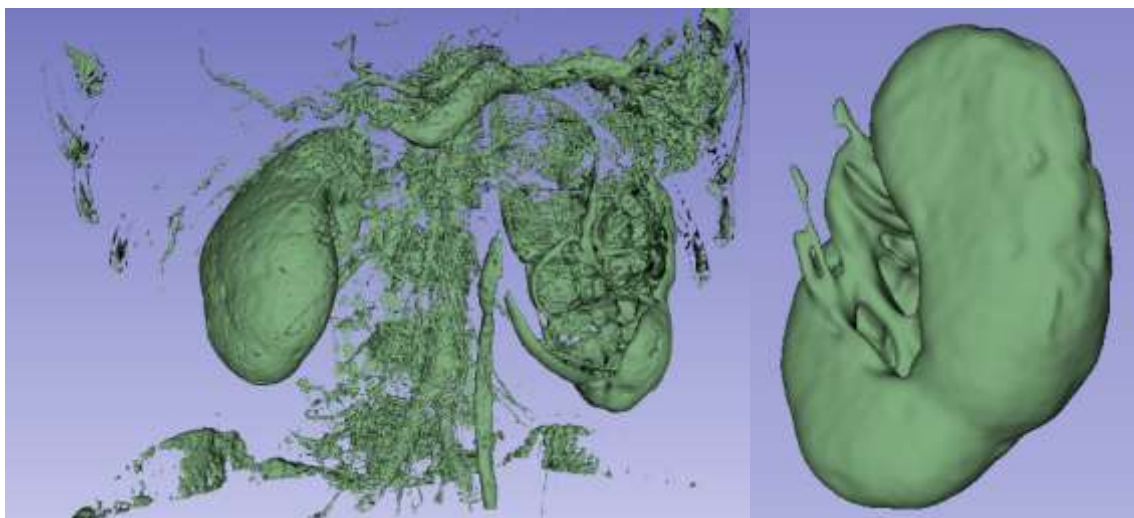


Figure 3.2: images of the threshlodging of the right kidney.

Arterial blood vessels were obtained through a Threshold of [172, 2948], figure 3.3. The Second step was to eliminate the undesired organs with the scissors, getting only the vessels. After that, the closing operation was done, several times to get the final model.

The **tumour** in the left kidney was segmented using Growing and Seeds, so two masks were created, to get the model. Both masks refer to the background of the structure

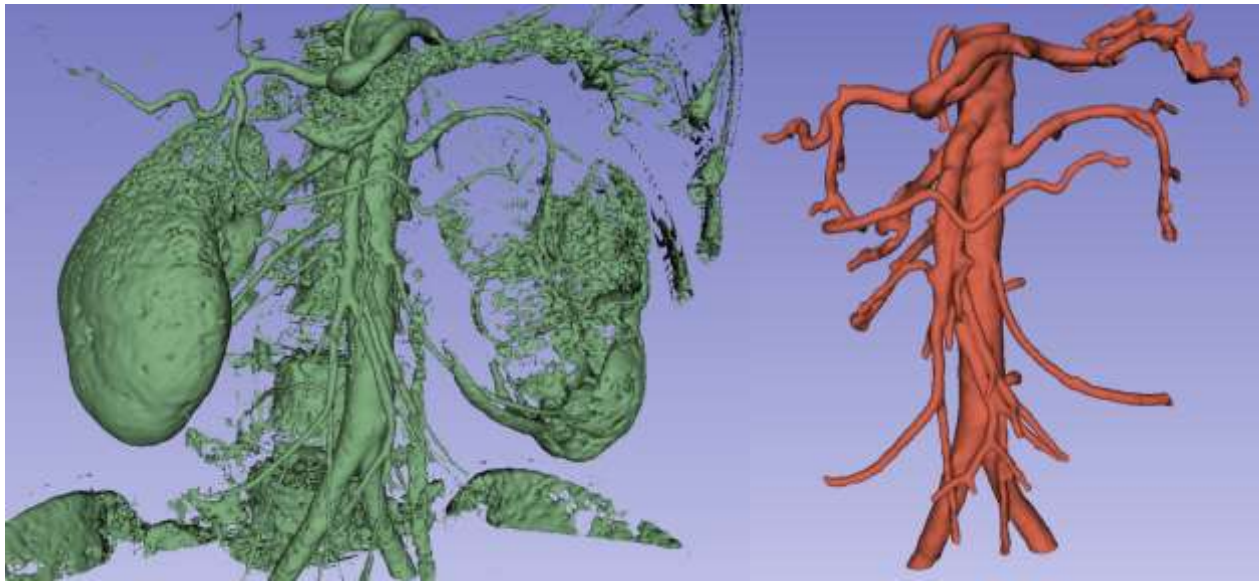


Figure 3.3:images of the thresholding for the artial vessels.

and the other to the inner part. This method was done, instead of using automatic tools as the color intensity of the tumour was confused with the contour. After applying the algorithm, a Gaussian filter with a $\sigma=1,5$ mm for three consecutive times. Figure 3.4

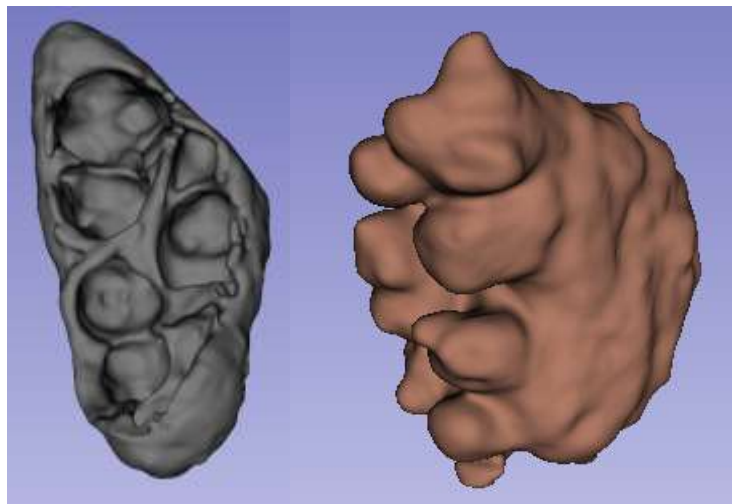


Figure 3.4: images of the left kidney and tumour.

Moreover, the structure linked to the tumour, the **left kidney**, was also developed through the Grow and Seeds algorithm, as during the practice, it appeared to be more

convenient than thresholding. Masks were implemented, changing the display to a threshold that only preserved its intensity, those in between a range of [-50, 150]. Finally, the surface was smoothed using a Gaussian filter of $\sigma=2$ mm. Figure 3.4

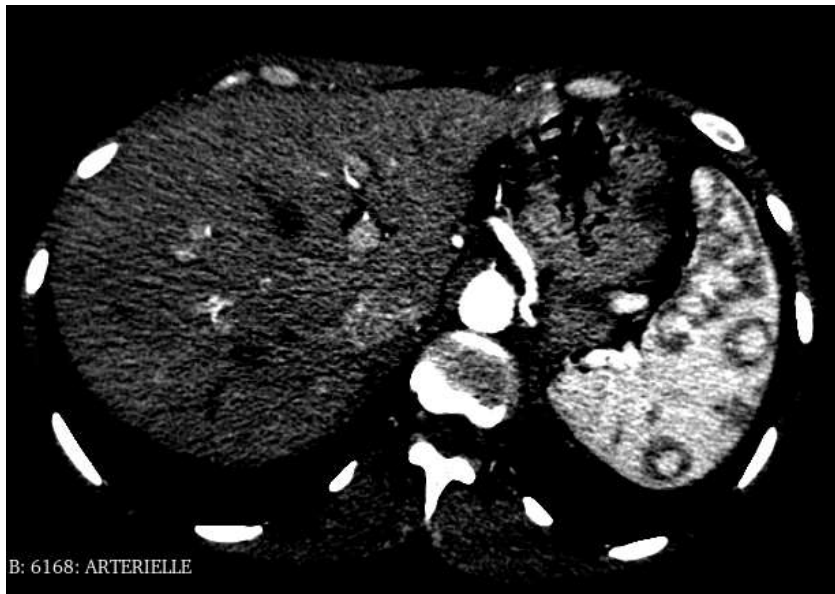


Figure 3.5: display of the sagittal view showing the kidney and the spleen.

Then it was segmented the **spleen**, for which the display was modified as in Figure 3.5. As in the last organs, the Grow from Seeds algorithm did the segmentation because it was less time-consuming than the thresholding and noise cancellation. After that, opening and Gaussian filter were applied with a structural element of 5x5x7 pixels and $\sigma=2$ mm, respectively. Figure 3.6

The display remained the same for the **gallbladder** as for the spleen, and Grow from Seeds using 14 masks among the slides where the organ appears. Surface smoothing was done using Closing with a structural element of 3x3x3 pixels, Opening with a Structural Element of 3x3x3 and a Gaussian Filter with a $\sigma=2$ mm. Within **Figure X** shows the Grow from Seeds technic, the model obtained and the final model after the smoothing process.

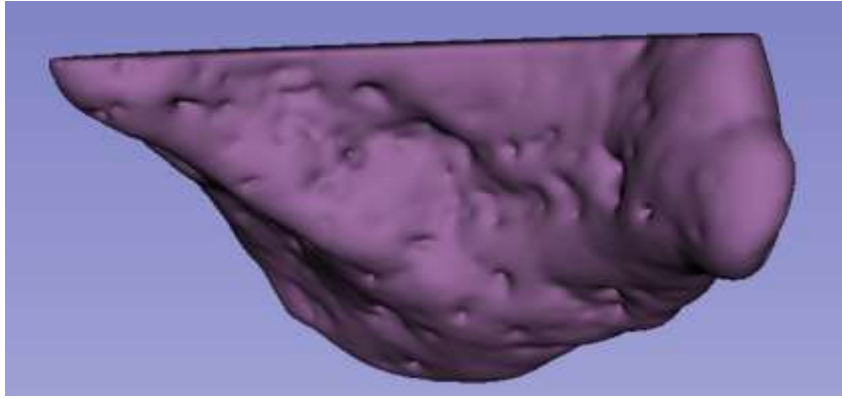


Figure 3.6: segment of the spleen.

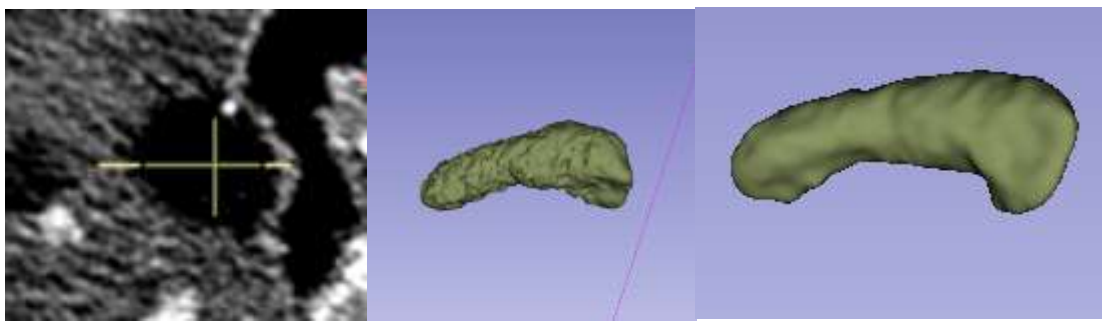


Figure 3.7: images of the algorithm grow from seeds, the original gallbladder and with the smoothed surface.

Continuing with the missing organs, the **liver** was segmented by changing the display, increasing the contrast of the edges as the intensity of the surrounding structures was similar. For the development of the masks, it was previously necessary to acquire anatomical knowledge about the structure of the liver, and its interpretation in a CT file. Moreover, the presence of some organs already segmented helped in the interpretation of the liver (Figure 3.8). The following steps were into creating the masks and emending the model, figure 3.9. Finally, the use of Opening and Closing morphological operators with a structural element of both 5x5x5 pixels, the model from figure 3.9 was achieved.

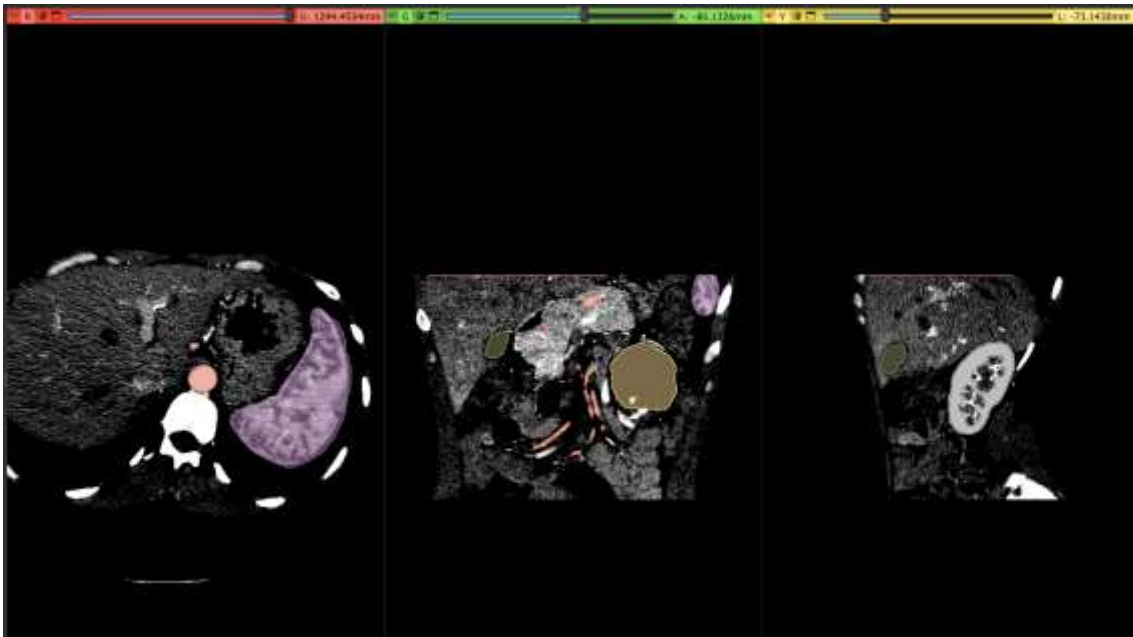


Figure 3.8: display of the three views modifying the pixel overview to heighten the liver.

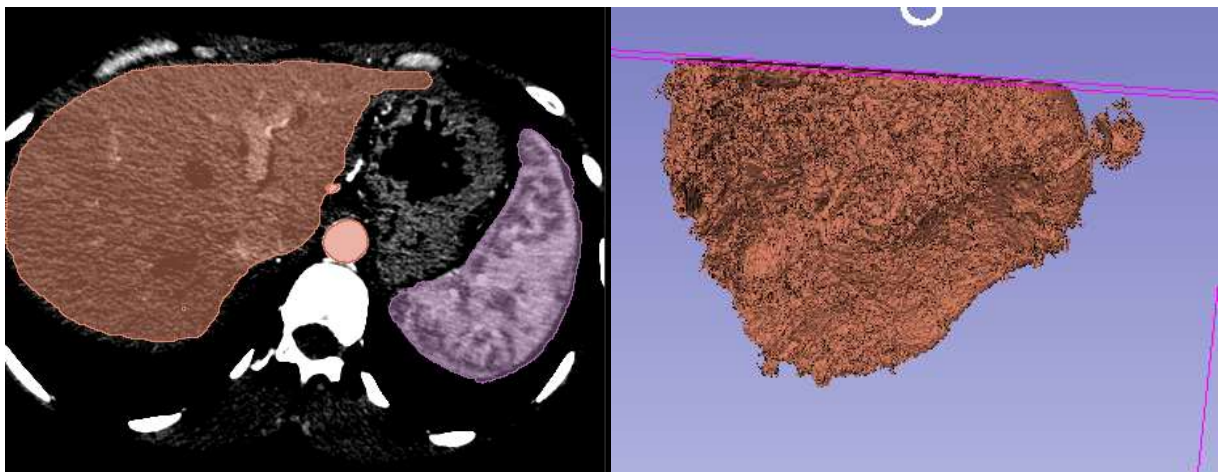


Figure 3.9: images of the segmented liver before and after implementing smoothing factors.

The **bones** were extracted by using a Threshold similar to their intensity [300, 600], as its value had a specific range, with that, also segmenting few organs that were already studied: Kidneys and arterial vessels; which were subtracted from the model the logical operation subtract, whose operation is to eliminate from the element A the element B. Finally, leveraging the scissors, to remove the radical dorsal spine arteries, and so on, Opening operations to get small noise in the surface out. Figure 3.10



Figure 3.10: segmented model of the bones.

For the **pancreas**, a Threshold was done with an interval of [75, 130], extracting most of the organ as its boundaries related to the rest of the anatomical structures were clear. After that, it was applied a Closing morphological operator with a 5x5x5 structural element and a Gaussian filter with a deviation value $\sigma=1,5$ mm. (Figure 3.11)

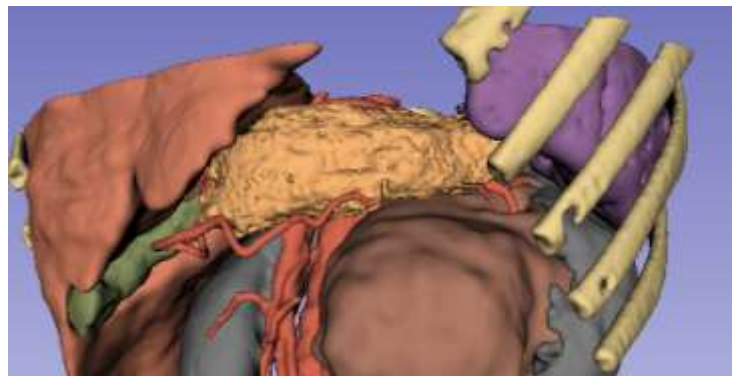


Figure 3.11: segmented model of the pancreas showing a display with the surrounding organs.

From now on, as the segmentation of the last organs required a more precise, some image smoothing filters were attempted, to smooth but retain the contrast edge. Some of them were: the Kuwahara filter [21] [22] done using Matlab program, not and some more basic, such as median, gaussian, gaussian adaptive. All to was to get a smoothed image to segment the stomach and the Cava.

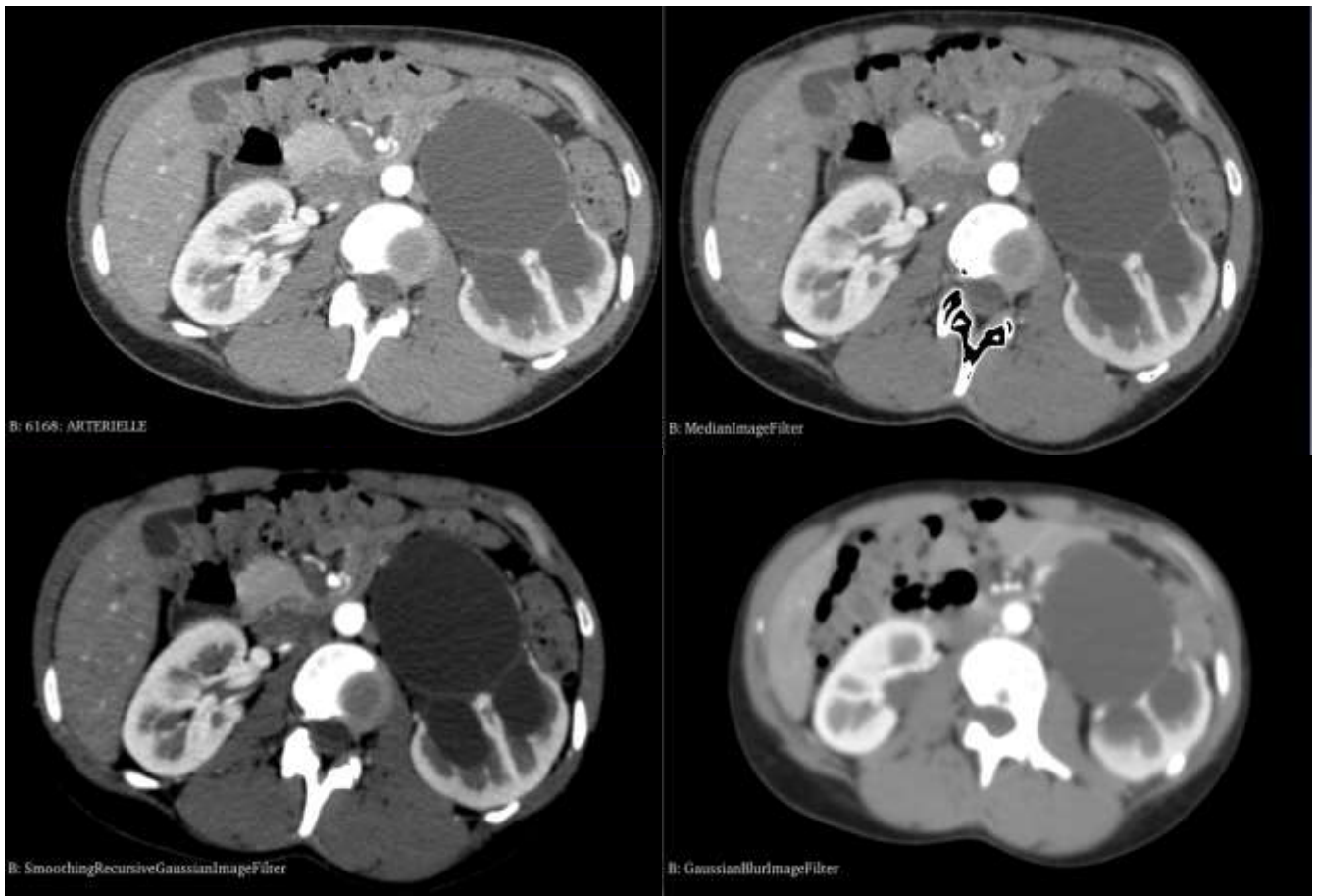


Figure 3.12: four display of a sagittal slide comparing different filters.

Therefore, to get the **venous system**, hence the cava and its branches and the porta, two different process were conducted. The display was modified selecting from a range of [-360, 580] and the MedianImageFilter was overlaid.

To get the **vena porta**: will use semi-hard tissue (30-150 threshold) subtracting what I have already done... and see what can I do to eliminate other organs and nose... Also painting with threshold (150-200) to signal those important venus, and another opening... to eliminate the small noise. Then we will use the scissors to eliminate big elements and hollow form medial surface (1,2mm or 2x2x2 pixel) to grow the segments in order to use the Joint Smoothing with a factor of 25%, and a Gaussian filter of 0,5 to suavize the surface. For those in the liver used painting with treshold between 0-60 and remake some parts up to 80 because it was really hard to segment It automatically. Later on, the smoothing part consistin of a Closing with a structural element of 3x3x3 pixels and an opening of 3x1x1 pixels.

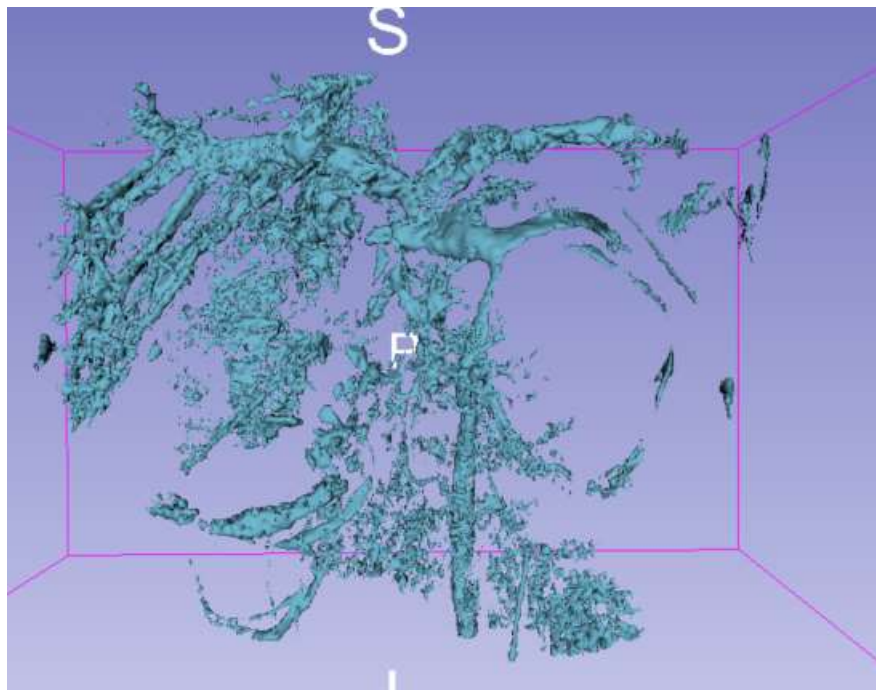


Figure 3.13: first display of the venus vessels segment.

The **venus cava**: due to the fact that it was really difficult to interpret it, considering a threshold around [60, 80], but so as the organs linked to it. Moreover, due to the fact that it expands among the body, it will be hard to use a Crop structure and apply a threshold; therefore, painting tool whitin a threshold around [50, 80] was implemented. Once the segmentation was done, the surface was overlaid with a Closing with a kernel of (2mm 3x3x3 pixels), because the structure was not compact. Later on, a Joint Smooth

was used, with a factor of 50% and a Gaussian filter $\sigma=1$ mm to eliminate abrupt changes.

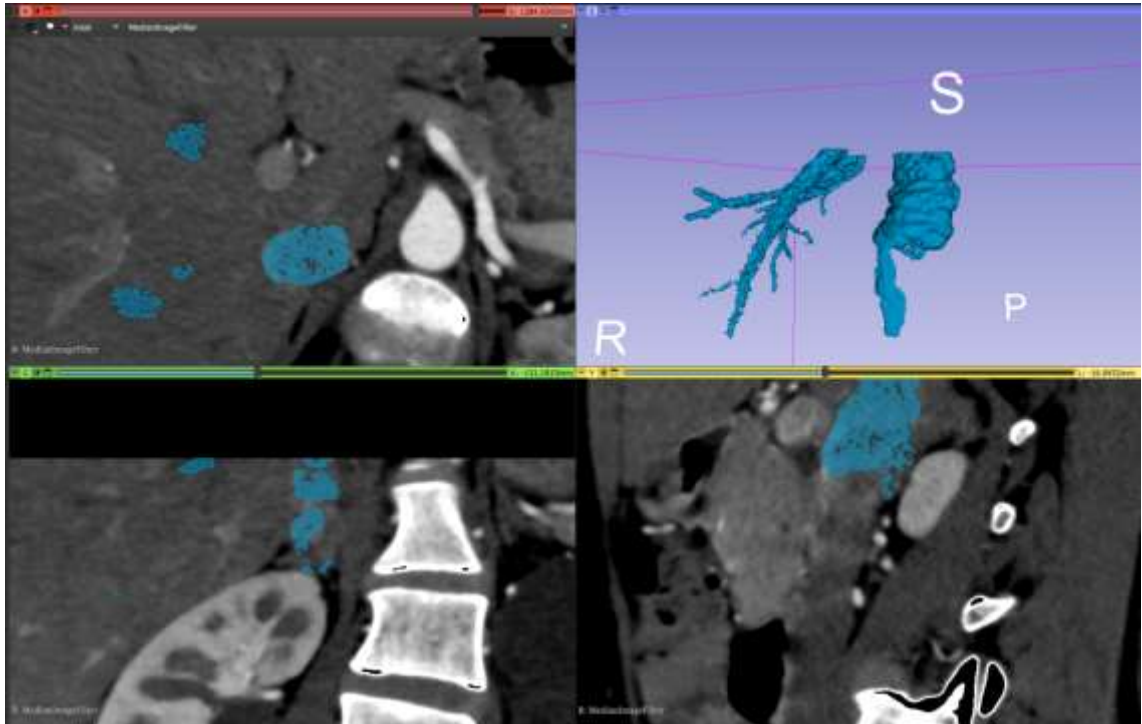


Figure 3.14: display of the different views and segment of the porta vena.

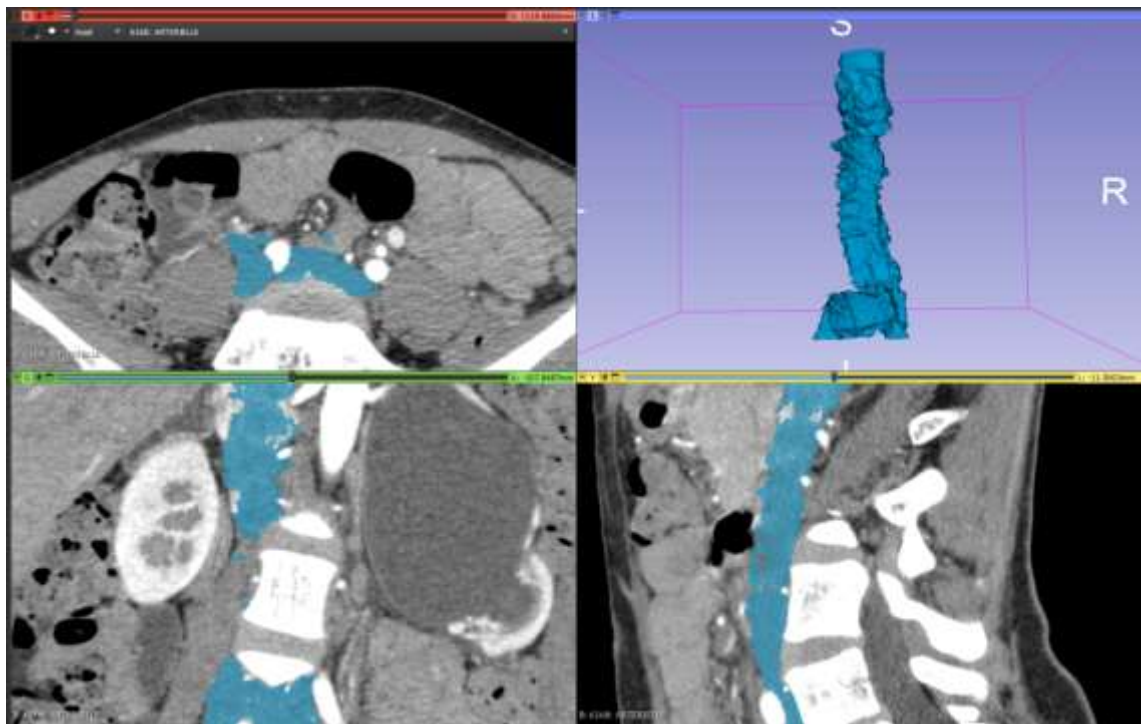


Figure 3.15 display of the different views and segment of the vena cava.

To get **stomach** segmentation, the display was the same as in the former organ, presenting many difficulties as it is surrounded by many organs and the inside is plenty of air; hence, it was not possible to extract by using intensity methods, but just painting the edges with a Threshold of [30, 150] manually considering that is made up of a muscular wall. Moreover, the surface was cleaned, removing islands of pixels included in the interval of the painting and subtracting the segmentation from the adjoining. As the wall thickness was up to few pixels, Grow Surface method had to be called with a margin of 1x1x1 pixels. Finally, the surface was filtered by a Gaussian with $\sigma=1$. Figure 3.16.

The **skin**, as it had a homogeneous intensity for being composed of the same kind of tissue, was extracted by applying a Threshold of [-100, 0]. In addition, some walls had holes due to its thinness; hence, a Closing with a structural element of 5x5x5 pixels was calculated and was smoothed by using scissors, as the Gaussian and Median generated holes.

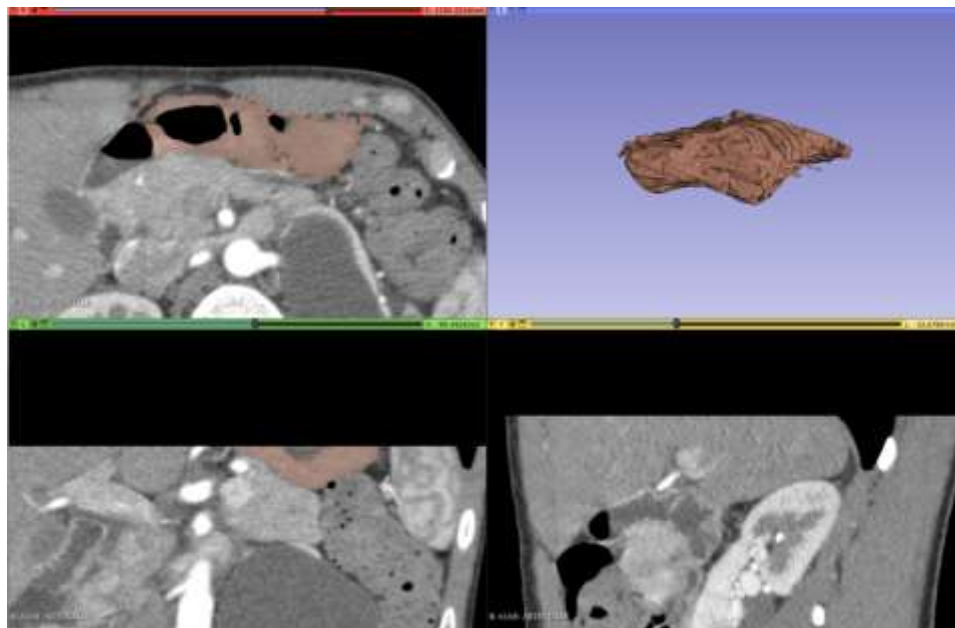


Figure 3.16: display of the different views and segment of the stomach.

3.2 Operation planning based on the FRS curriculum list.

As this work aimed to develop a realistic RAMIS, simulating a partial nephrectomy, an operation plan of the procedure was done following the FRS curriculum list of concepts. Performing the simulation using a daVinci® surgical robot integrated with the open-source dVRK [23], being connected to the teleoperation console of the dVRK and the real Patient-Side Manipulators (PSMs). Moreover, a 3D viewing capability is provided by the High-Resolution Stereo Viewer (HRSV), having their feed sent independently on the left and the right oculars of the console, getting a three-dimensional perception of the virtual environment.

The partial nephrectomy consists of the excision of a partial section of the kidney, due to diverse causes, but mainly malignant tumours having to be removed. There are eight general steps during the surgical procedure focusing on the sixth and the seventh, for which the renal hilum is clamped and the tumour excised. Regarding the other tasks, due to physical limitations and not the necessity to replicate an exact model, will not be simulated.

By replicating the clamping of the hilum vessels, the surgeon intends to clog the blood to the kidney, preventing bleeding during the resection of the carcinoma. The phantom will reproduce this task by splitting the blood vessels from its adjacent anatomical part. Therefore, the gonadal vein is unstuck from the renal vein, and so on, the renal vein from the cava. On the other side, the arterial system is clamped by removing the capsular renal branch and the suprarenal artery from the aorta. Finally, the excision of the carcinoma is represented by its division of the right kidney, by this also engaging the competences already mentioned.

These exercises pair the FRS curriculum as the user will practise the surgical skills present on the list, such as: the camera control, moving around the environment to grab the vessels. Another robotic surgical concept exercised is clutching, since moving the MTMs is compulsory whilst the procedure. Moreover, multi-arm control and eye-hand instrument coordination are skilled by splitting the vessels; due to that, both MTMs need to be positioned so that one grabs a vessel and the other is pulled. In addition, wrist

articulation is also trained for the same reasons as the former and atraumatic tissue handling is practised by picking and dropping the vessel. **Table 3.1**

<i>Tasks</i>	<i>Vessel Removal</i>				<i>Excision</i>
<i>Anatomical structure</i>	Gonadal vein	Renal vein	Suprarenal Artery	Capsular Renal Branch	Tumour
<i>Important factors</i>	Appropriate position of the PSMs for the completion. This action is simulated by the disconnection of the magnets that join the re with the renal.	Appropriate position of the PSMs for the completion. This action is simulated by the disconnection of the magnets that join the renal and the cava.	Appropriate position of the PSMs for the completion. This action is simulated by the disconnection of the magnets that join the suprarenal with the aorta.	Appropriate position of the PSMs for the completion. This action is simulated by the disconnection of the magnets that join the branch with the aorta.	Using the tip of the PSMs to lift the tumour from the kidney. By the time the two magnets placed on the edges of the tumour are removed, the count will conclude.
<i>FRS curriculum</i>	Camera control Clutching Multi-arm control Eye-hand instrument coordination Wrist articulation Atraumatic tissue handling	Camera control Clutching Multi-arm control Eye-hand instrument coordination Wrist articulation Atraumatic tissue handling	Camera control Clutching Multi-arm control Eye-hand instrument coordination Wrist articulation Atraumatic tissue handling	Camera control Clutching Multi-arm control Eye-hand instrument coordination Wrist articulation Atraumatic tissue handling	Camera control Clutching Multi-arm control Eye-hand instrument coordination Wrist articulation Atraumatic tissue handling

Table 3.1: description of the tasks and explanation of each task simulated.

3.3 Adapting the 3D-model printable, according to partial nephrectomy and FRS tasks

After obtaining the segmentation of the CT file, it had to be decided which organs get involve in a partial nephrectomy, and later on modify the real features of the model, previously to its exportation to the 3D printer, to guarantee the success of the printing process.

In this sense, the organs involved in the surgery and hence, printed, were: the right kidney, pancreas, stomach, left kidney, tumour, skin and circulatory system. As shown in the images below, the organ's surface was smoothed by Gaussian and Median filters having a loss of surface reality, but achieving a faster print and less use of material. Moreover, the arteries and the venas were simplified by selection those vessels directly intervening on the surgical scenario, therefore, remaining the aorta, the suprarenal artery and the arterial capsular branch; on the other side, the cava, the gonadal and the renal veins. Figure 3.17, Figure 3.18, Figure 3.19

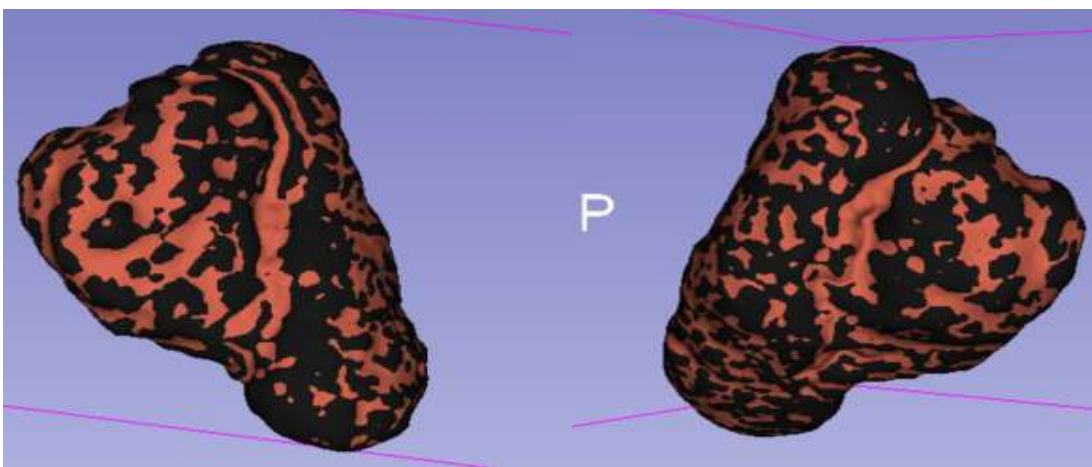


Figure 3.17: image of the tumour smoothed, in black the removed surface.

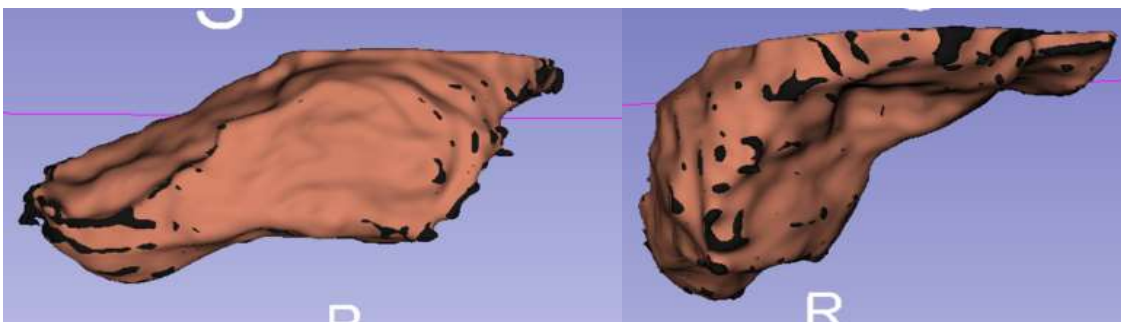


Figure 3.18: image of the stomach smoothed, in black the removed surface.

The second part is related to the docking of the PSMs into the phantom. Levering the segmented skin from the previous file, following the standard positioning of the insertion instruments, it was designed two possible scenarios, nonetheless, the idea of the project is to simulate a partial nephrectomy, but with this, the idea is to get used

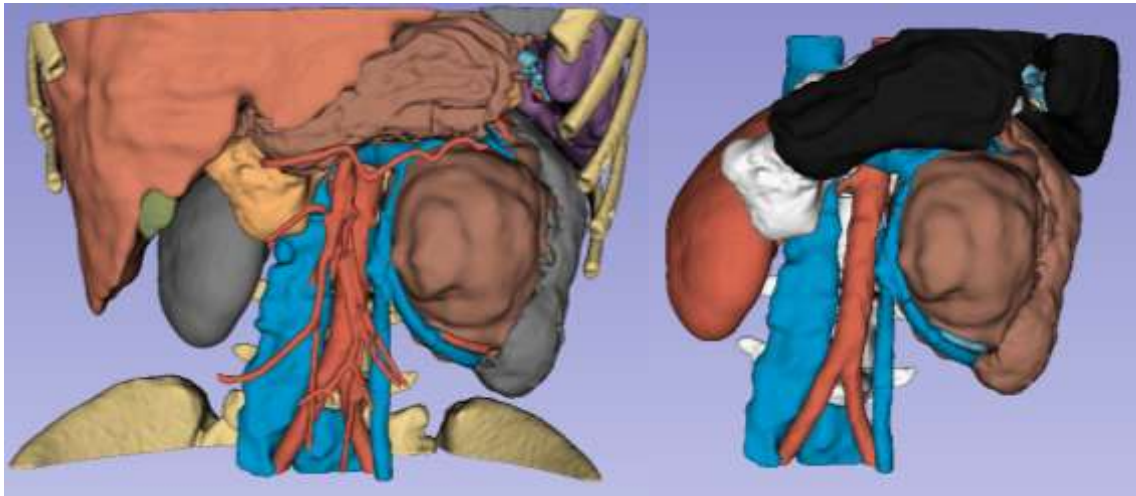


Figure 3.18: comparative of the original and printable model.

to the docking training, and for future different approaches. The first one consist of a general surgical scenario, whose inserction points are referred to the central womb are. The position of the tools in the second scenario would be used in a partial nephrectomy, so that the camera would be placed in the hole closest to the pelvic area, the left MMP in the internal area and the right MMP in the external area. Finally, as seen in **Figure X**, the inserction points have a radius of 30mm and the distance is equidistant for each three pair of holes, spaced at 80mm.

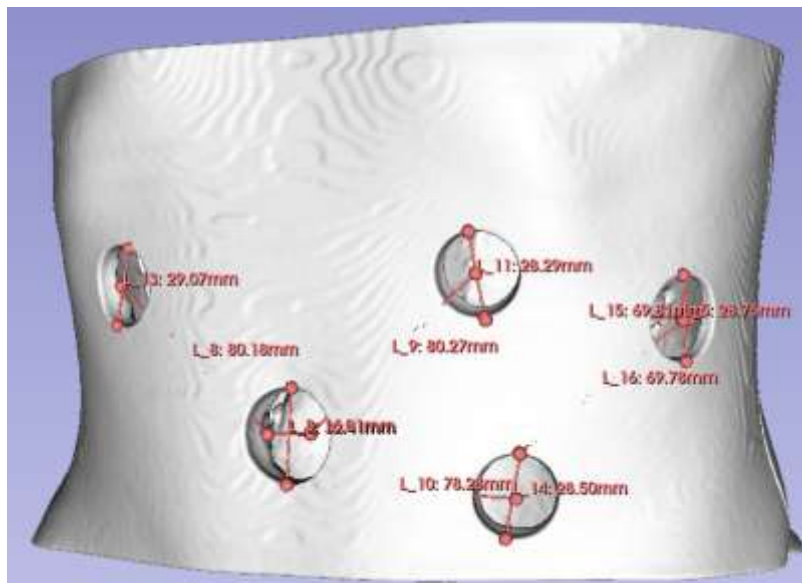


Figure 3.19: image of the docking holes for the partial nephrectomy. [24]

3.4 3D printing

The 3D printing aim was to approximate the texture of the simulated organs to the real ones. This section searches to describe the characteristics of each part that was printed considering the limitations inherent to 3D printing, bearing in mind that there was no previous knowledge on this field. The printer used is the UltimateMaker S3, with a nozzle diameter of 0.4mm, and the program for the completion of the 3D file is UltiMaker Cura version 5.2.2. The previous segmentation of the model was exported as a .STL file from 3D slicer.

As a way of starting, among the parameters modifiable for the printing were selected: the type of material (available in the da Vinci Nearlab), the support material, infill density, wall line count, the layer height and the retraction distance. Within the type of material, infill density, internal structure, and wall line count the softness and stiffness to the organ but also, as an important consideration the time of print. Whilst, the support material characterized the cleanliness in the surface, the layer height reflects the precision in details; and finally, the retraction distance solved the plastic fluff on the surface.

The right kidney, was printed using Red TPU (thermoplastic polyurethane) 95A with an infill density of 5.0% and a gyroid pattern, with a wall line of 3 providing a firm touch, furthermore using Breakaway as support which was found to be difficult to remove. The pancreas and spleen were printed on the same way as the kidney but changing the infill density to 0.0%, in order to get the texture expected, also, by implementing 4 wall line count to guarantee the success of the printing, and the support material was changed to PVA, therefore, removing it easier. Furthermore, for the stomach it was adjusted the layer height to 0.12mm, expecting a better detailed print, but it appeared some defects.

In addition, the left kidney was printed using a pad of 5.0% by reason of the complex structure of the calyces in the kidney, using a gyroid pattern and a wall line count of 3, achieving a promising result, in part by changing the retraction distance to 9 mm avoiding plastic fluffs. For printing the vertebrae, it was used white PVA, which is a rigid material, closer to the real texture of the bones and an infill of 5.0% using a gyroid

structure using a layer height of 0.15mm, not searching proper resolution quality but for the success of the print, finally using a 2 wall line count.

Finally, the arterial system was printed the same way as the left kidney and the venous using Blue ABS, as it was the blue material resting on the laboratory, modifying the wall line count to 2, as it was a rigid material, and therefore, the success of the print was guaranteed.

Organs	Right kidney	Pancreas	Spleen	Stomach	Left Kidney	Vertebras	Arterial system	Venous system
Material	Red TPU 95A	White TPU 95A	Black TPU 95A	Black TPU 95A	Red TPU 95A	White PVA	Red TPU 95A	Blue ABS
Support material	Breakaway	PVA Filament Natural	PVA Filament Natural	PVA Filament Natural	PVA Filament Natural	PVA Filament Natural	PVA Filament Natural	PVA Filament Natural
Infill density	5.0%	0.0%	0.0%	0.0%	5.0%	5.0%	5.0%	5.0%
Infill pattern	Gyroid	Null	Null	Null	Gyroid	Gyroid	Gyroid	Gyroid
Wall line count	3	4	4	4	3	2	3	2
Layer height	0.13 mm	0.13 mm	0.13 mm	0.12 mm	0.13 mm	0.15 mm	0.13 mm	0.13 mm
Retraction distance	6.5 mm	6.5 mm	6.5 mm	6.5 mm	9 mm	9 mm	9 mm	9 mm

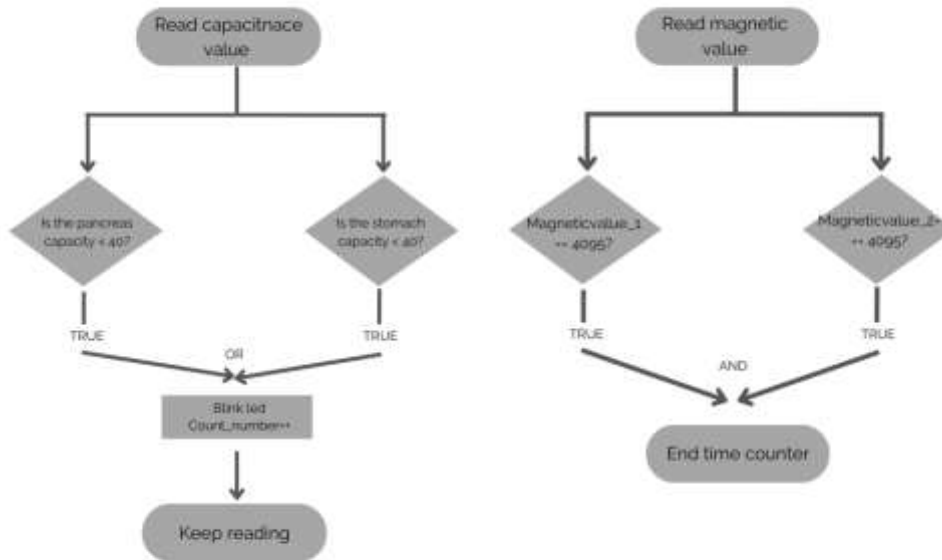
Table 3.2: simplification of the printing parameters for each of the printed organs.

3.5 Sensoring and performance metrics

As part of this work, data collection from the tasks appears crucial for assessing the expected tasks. This data recompilation described in figure 3.20 is split into different branches: sensing, data bus and display of the information.

Firstly, the data will be gathered by two A3144 Hall sensors, since the tumour holds two magnets in both tips, and the sensors are implemented in the calyces of the right kidney matching with the magnets, intending to register the time it takes the user to simulate the excision, by previously having pressed a button that starts counting. The other sensor implemented is a capacitive sensor provided by the Microcontroller ESP32, which lights on a Led Light and increases the count of the number of touches, when the capacitance decreases to a certain value, as shown in scheme 3.1. Moreover, the time

spent for the execution of each of the tasks, hence, the removal of the vessels, will be recorded by an external timer. **Table X**



Scheme 3.1: algorithm of the blinking and touch counting process.

Moreover, considering the perception of the users after the testing is also an optimal variable to ensure the proper skill improvement while using the ROMIS, as a way of assessing the surgeon's confidence in the tasks provided. Thus, a Google Forms is conducted among the users, by answering seven different questions; the first two regard the dominant hand and the previous level of experience and the rest are related to the tasks the subjects are implementing within the exercises.

All sensors recently commented are connected to ESP32 Microcontroller, leveraging for its manipulation the Arduino IDE program (v2.1.0, Arduino®), which processes the information using C++ language managing low- and high-level signal processing, calculates the results and communicates with the Arduino IDE by means of serial connection (USB port) run from the computer. Furthermore, after the Arduino platform, the removal time of the excision, and the touch number count are sent to a Visual Studio platform (v2022, Microsoft®), which will create a .csv file where to store the data. Figure

3.20

Finally, all the information is aggregated into the .csv file providing data to assess the learning surgeon. This level of automatization in measuring searches to preserve the data from human measuring errors and guarantees that the metrics are logged in the same way for all subjects.

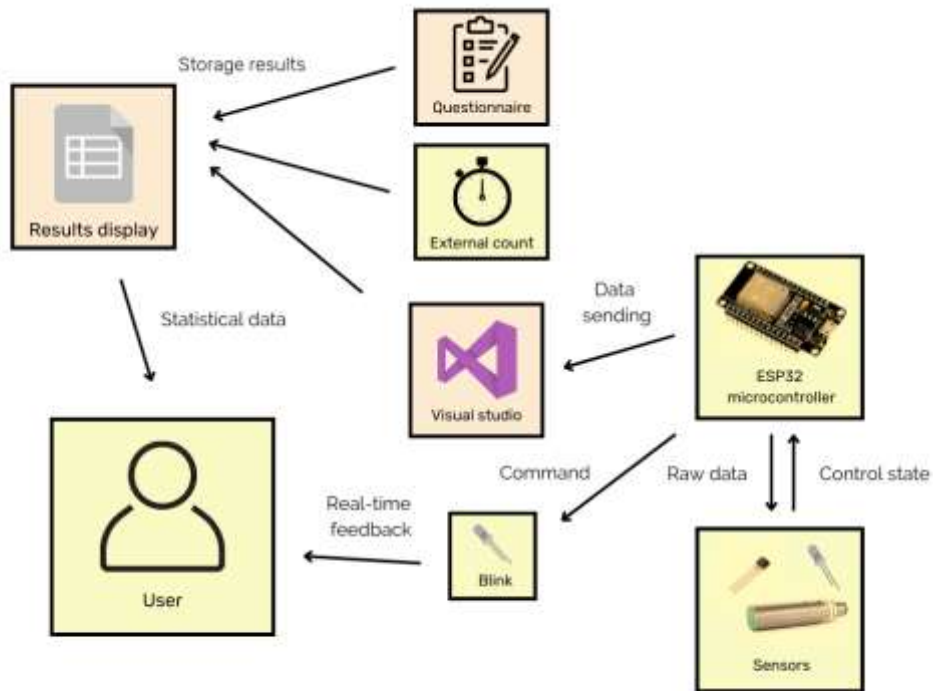


Figure 3.20: workflow of the data collection and storage.

Tasks	Vessel Removal				Excision
Anatomical structure	Gonadal vein	Renal vein	Suprarenal Artery	Capsular Renal Branch	Tumour
Measured Metrics	Time Contact count	Time Contact count	Time Contact count	Time Contact count	Time Contact count
Sensors and methods	External timer Capacitive proximity sensor	External timer Capacitive proximity sensor	External timer Capacitive proximity sensor	External timer Capacitive proximity sensor	Hall-sensor Capacitive proximity sensor
Real-time feedback	Led blink	Led blink	Led blink	Led blink	Led blink
Forms doc.	Questions on a scale from 1 to 5	Questions on a scale from 1 to 5	Questions on a scale from 1 to 5	Questions on a scale from 1 to 5	Questions on a scale from 1 to 5

Table 3.3: simplification of the sensors and variables measured within each of the tasks.

3.6 Evaluation metrics

The data logged in the .csv file will need to be displayed properly, in a way of assessing the user after the training, but also, as part of the validation work, to probe that performance metrics are properly measured.

Data is studied by performing a Box & Whisker plot in each of the attempts for the 5 removals proceeded in the experimental phase. The metrics are obtained from the main statistical fundamentals of the Box & Whisker plot, hence:

- Mean: this parameter approaches the common time performed by the volunteers during the experiment, understanding, hence, whenever a patient has more or less difficulties in the realisation of the task.

Being $j = \{1, 2, 3\}$ the number of attempts and given an array of n elements the number of volunteers: $\{x_1, x_2, \dots, x_n\}$

$$\bar{X}_j = \sum_{i=1}^n \frac{x_i}{n}$$

- Median: criteria that takes into account the variability of the data since knowing the upper and lower half of the results. This data, regarding the Box & Whisker plot, shows the uniformity or heterogeneity of the time.

For an ordered data list of n elements: $\{x_1, x_2, \dots, x_n\}$

$$Median = \frac{x_{n+1}}{2}$$

- The standard typical deviation (STD): explaining, in a different way, how dispersed the data is in relation to the mean. Nonetheless, this parameter can be influenced by the skill learning rate of each user and the previous knowledge of the a daVinci® surgical robot controls.

Given an array of n elements: $\{x_1, x_2, \dots, x_n\}$

$$\sigma = \sqrt{\frac{\sum(x_i - \bar{x})^2}{n - 1}}$$

Finally, the metric considered that implements the previous statistical parameters is the variation, or increasment in percentage, of the time between the first and the third attempt for each task measured, and the three statistical metrics derived from the Box & Whisker plot. Therefore, obtaining a new criteria to ases the performance of the user.

- Variation: gives a simple comparison between two parameters, in this case, the evolution of the $\bar{X}_j, Median, S$ during the attempts. By this, the progress of the learning can be evaluated.

$$Variation\ in\ percentage\ i = \left(\frac{x_{1,i}}{x_{3,i}} - 1 \right) \cdot 100$$

Being the subset $i = \{ \bar{X}_j, Median, S \}$

Regarding the Google Form query, it consists of a seven simple questionnaire in which they can be answered on a scale from 1 to 5, from lower to higher. It begins by asking the dominant hand and the level of control with the da Vinci had previosly to the experiment. The following questions applie one of the conceptual surgical tools intended to be evaluated in this work (*hand-eye coordination, clutching, wrist articulation, multi-arm contron and atraumatic tissue handling*), and the last one assess the utility of real time feedback sensor. The questions are:

- 1) Do you feel an improvement moveing the da Vinci arms more accurately, over the attempts?
- 2) Do you feel an improvement in moveing the camera, over the attempts?
- 3) Do you feel an improvement manipulating both da Vinci arms, at the same time, over the attempts?
- 4) Do you feel an improvement in using the clutch button, over the attempts?
- 5) Do you think the visual feedback (red led light) encouraged you to be more accurate moveing the PSMs?

3.7 Experimental protocols

As the surgeon's training and assessment is the key objective of this work, the experimental phase aims to evaluate the effectiveness and benefits of the phantom developed. Hence, an experimental study was conducted among some novice users.

For this aim, the experiment was conducted on a decommissioned first-generation daVinci® surgical system from 2016. The system is retrofitted with the dVRK [25] (daVinci® Research Kit) framework, an open-source mechatronics system comprising electronics, firmware, and software. The dVRK, is built on a ROS (Robot Operating System) framework, providing convenient access to the sensors, actuators, and control algorithms of the daVinci® robot.

A group of 12 volunteers was asked to execute the surgical tasks over three repetitions. Considering that the scope is to assess, giving a real-time feedback and ensure proper learning, the experiment was divided into three attempts in order to appreciate a possible variation in their performances. However, after the experiment, a questionnaire was conducted among the volunteers to evaluate their confidence in using the *daVinci*® robot, but also to consider the task's difficulty and consider future modifications and implementations.

Subjects were 17% females and 83% males, between 22 and 30 years old and all right-handed, among which some of them have had some previous experiences with the *daVinci*® robot; aspect being considered during the result analyses among the questions conducted in the Google Form document.

The experiment order consisted of encouraging the subject to remove the gonadal vein first, followed by the renal vein, the suprarenal artery and finally, the capsular branch. Once, the clamping phase was done, it was asked to remove the tumour from the kidney and place it out of the body, repeating these tasks three times.

In this study case, it has yet to be evaluated whether the user has internalised the skills learnt to adapt them to real surgical scenarios, which is known as *Skill Transfer*. Neither guaranteeing *Skill Retention*, by overtrained users by replicating the same tasks, nonetheless, the subject were encouraged to find their way to carry out the tasks.

3.8 Ethical considerations

During the project, ethical aspects have been considered regarding the design of the overall work. Hence, anonymity in CT DICOM files has been preserved, therefore safeguarding the privacy of the patient involved and preventing unauthorized disclosure of his personal information. Moreover, during the experimental training, its has been guaranteed the privacy of the 12 volunteers during the experimental phase, respecting their rights to confidentiality and minimizing potential harm or breaches of trust. In addition to these measures, other ethical considerations have been addressed. These include obtaining consent from the participants, ensuring the fair distribution of benefits and risks, maintaining data security and confidentiality throughout the project, insuring that rhe . By demonstrating a commitment to ethical conduct and responsible data handling, the researcher upholds the integrity and validity of the project, contributing to the advancement of the research while protecting the rights and well-being of all involved parties.

Chapter 4

4. Results

In this section the results of both the 3D printing and the experimental phase within the phantom will be exposed, discussing them in the following chapter.

4.1 3D printing results

During the organs 3D printing process, there was an increasing progress for which errors were solved by facing errors during the exercise. Regarding some difficulties, the balance between material and time expenditure were the challenging variables through the project, but also the intention of simulating the texture of the organs by modifying the layers, therefore, finding a balance between the stiffness and the completion of the print; having into consideration the plastic fluff and cleanliness of the surface.

The final results, doing a comparison between the settled model by Ultimaker Cura program and the result of the printed organs, are:

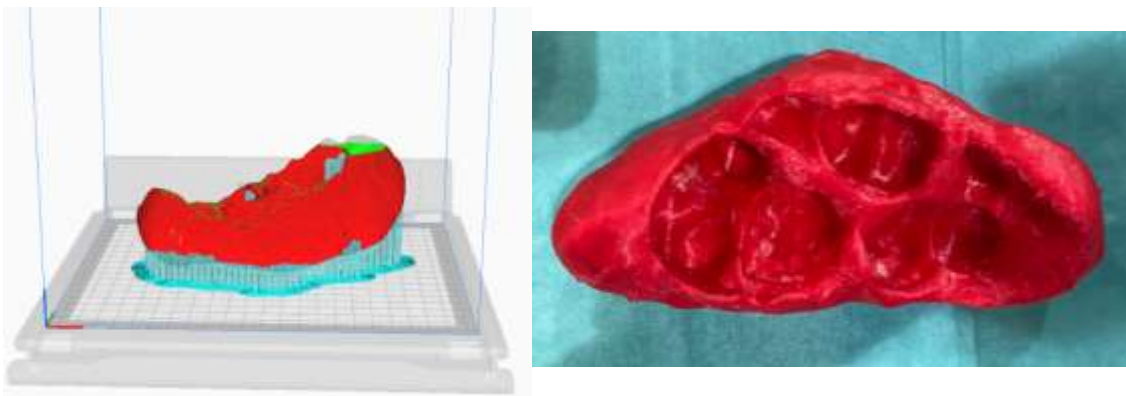


Figure 4.1: image of the printable left kidney, on the left, and image of the printed left kidney, on the right.



Figure 4.2: image of the printable pancreas, on the left, and image of the printed pancreas, on the right.

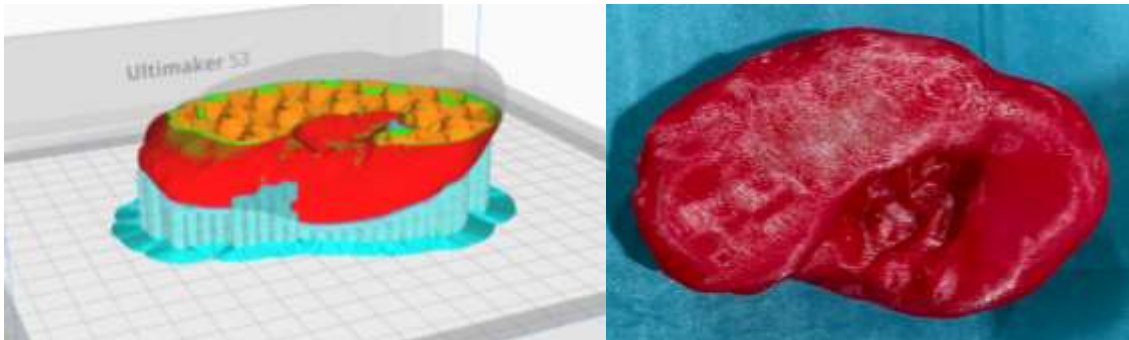


Figure 4.3: image of the printable right kidney, on the left, and image of the printed right kidney, on the right.

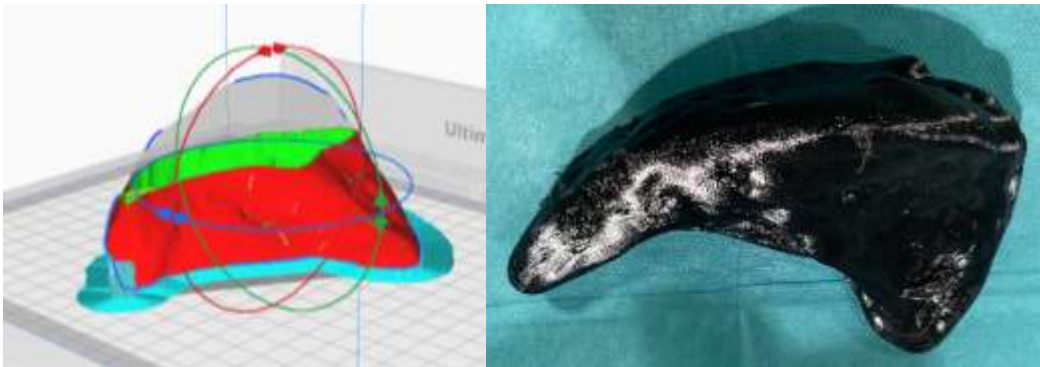


Figure 4.3: image of the printable spleen, on the left, and image of the printed spleen, on the right.

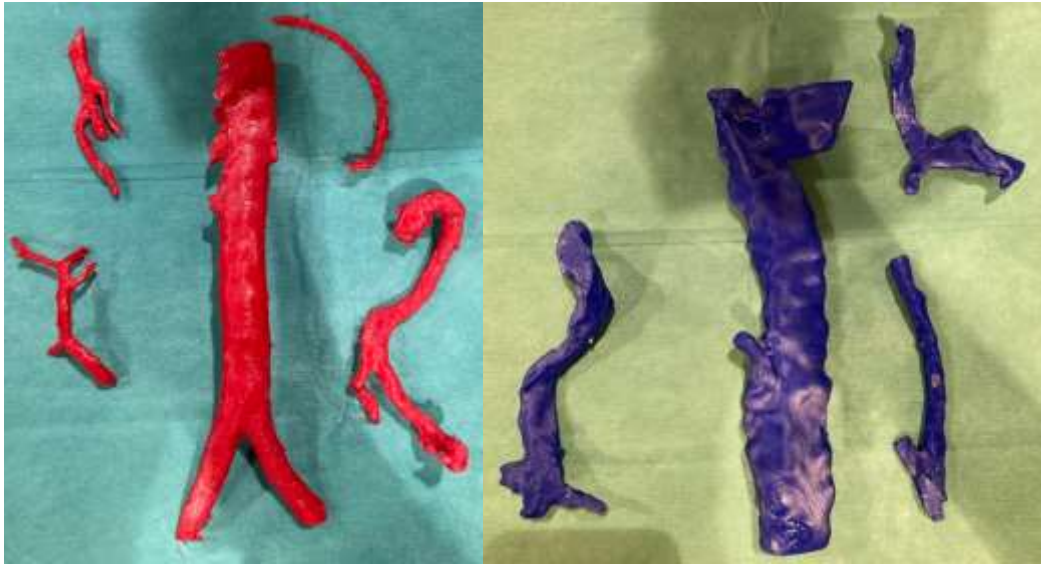


Figure 4.4: image of the printed artial vessels, on the left, and image of the printed venous vessles, on the right.

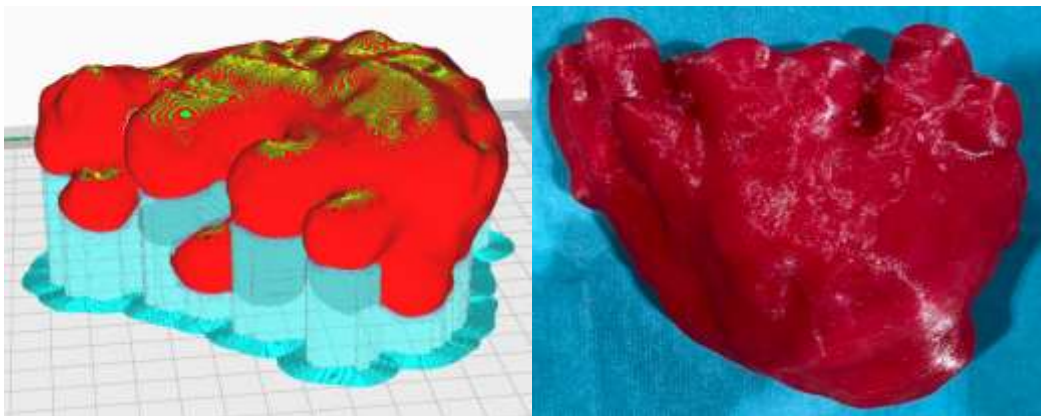


Figure 4.5: image of the printable tomour, on the left, and image of the printed tumour, on the right.

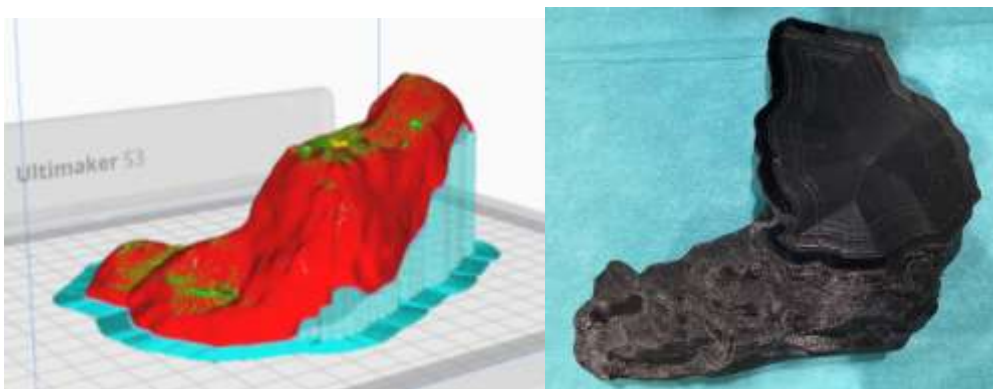


Figure 4.6: image of the printable stomach, on the left, and image of the printed stomach, on the right.

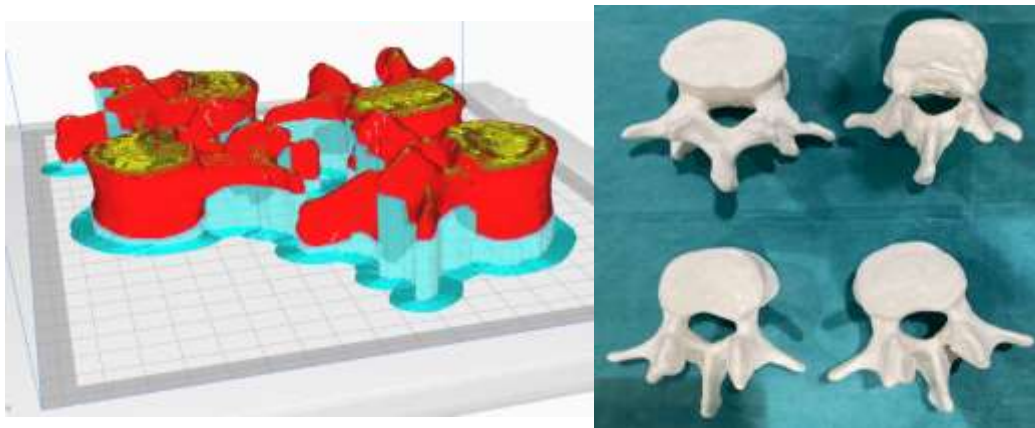


Figure 4.7: image of the printable column, on the left, and image of the printed column, on the right.

4.2 Results from the experimental phase

Graphic 4.1 shows the performance time of the five tasks: *gonadal and renal vein, capsular arterial branch and suprarenal and kidney removals*; and the number of times, both the pancreas and stomach were touched, during the removal of the capsular branch.

Regarding the assumption stated in this work, it is seen that within the attempts of the removal, time decreases, in three of the five tasks, and so does the count. In this sense, it is also relevant, taking into consideration the standard deviation of the time, as it reduces from the first to the third performance meaning that the distribution of the time, among the subjects, is more homogeneous, even though not all of them had the same previous knowledge of controlling the surgical robot, as seen in graphic 4.1, hence, getting to the idea that those with lower skill level were attempting to reach those volunteers with higher previous skills. According to the outcomes, in order to preserve the amount of data obtained, as it is twelve people; they were kept, concluding that in some cases, one or two of the subjects got higher records, specially in the first and second attempt.

The figure showing the the number of touches among the tries, shows an decrease of the amount which means that the PSMs are manipulated with further control respect

to the first approach. Considering that the removal of the arterial vessel was up to few centimeters close to both organs and there was no direct vision. Furthermore, the standard deviation which decreases from $\sigma_1 = 1.51$ to $\sigma_3 = 0.75$, probes that the results become homogeneous, achieving the same conclusion as in the previous commented tasks.



Graphic 4.1: from upper left to lower down each, representing the variables through the attempts.

Quantitative results are reported in the tables below, which for each of the tasks the mean, standard deviation and the median compared among the performances. Firstly, by considering the evolution of the mean, the tenacity for developing the tasks can be analysed. As seen in the results below, except for the suprarenal artery that increases the mean time, in the rest of the tasks the time decreases. Moreover, considering the median, as a relevant parameter, it is also seen that the variation from the first attempt to the third, reduces the time distribution of the tasks, concluding that during the attempts, subjects enhance their skills.

Furtermore, analyzing the results poised from the Google Form, the 60%-80% of the answers rated between 4-5 their perception of improvement in: *hand-eye coordination, clutching, wrist articulation, multi-arm contron and atraumatic tissue handling*. Showing a increase of confidence and sense of capabilitie, measured by the formulated questions but probed by the quantitative data above.

Removal metrics of the Gonadal Vein			
	Mean	STD	Median
Attempt 1	24.18	17.09	18.73
Attempt 2	22.54	13.27	16.13
Attempt 3	13.07	12.95	3.76
Variation (%)	85.02%	31.96%	398.14%

Table 4.1: representation of the mean, STD and Median for the gonadal vein.

Removal metrics of the Renal Vein			
	Mean	STD	Median
Attempt 1	20.15	15.62	16.63
Attempt 2	17.93	17.63	9.96
Attempt 3	10.32	6.48	9.39
Variation (%)	53.94%	7.32%	59.05%

Table 4.2: representation of the mean, STD and Median for the renal vein.

Removal metrics of the Suprarenal artery			
	Mean	STD	Median
Attempt 1	17.84	10.52	16.85
Attempt 2	16.87	15.29	11.64
Attempt 3	23.61	17.34	15.98
Variation (%)	-24.45%	-39.33%	5.44%

Table 4.3: representation of the mean, STD and Median for the suprarenal arthery.

Removal metrics of the Capsular Branch			
	Mean	STD	Median
Attempt 1	35.65	16.68	31.03
Attempt 2	24.27	15.00	28.80
Attempt 3	32.49	23.98	25.45
Variation (%)	9.73%	-30.42%	21.93%

Table 4.4: representation of the mean, STD and Median for the capsular branch.

Removal metrics of the Kidney			
	Mean	STD	Median
Attempt 1	88.14	60.28	75.80
Attempt 2	52.26	50.47	32.62
Attempt 3	58.08	44.17	53.85
Variation (%)	51.75%	36.49%	40.76%

Table 4.5: representation of the mean, STD and Median for the kidney.

Which previous controlling knowledge of the da Vinci Surgical Robot, on a scale from 1 to 5, you consider to have before the training?
10 respuestas

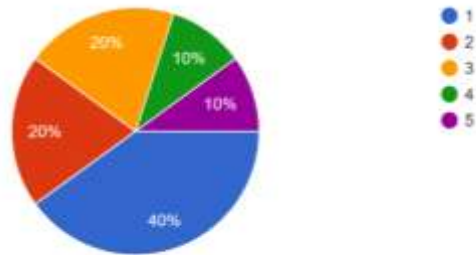


Figure 4.8: data collected from the question 1 of the questionnaire.

Do you feel an improvement manipulating both da Vinci arms, at the same time, over the attempts?
10 respuestas

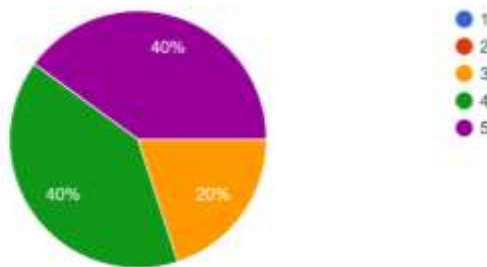


Figure 4.9: data collected from the question 2 of the questionnaire.

Do you feel an improvement in using the clutch button, over the attempts?
10 respuestas

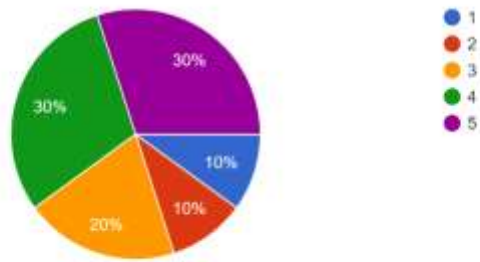


Figure 4.10: data collected from the question 3 of the questionnaire.

Do you feel an improvement in moving the camera, over the attempts?
10 respuestas

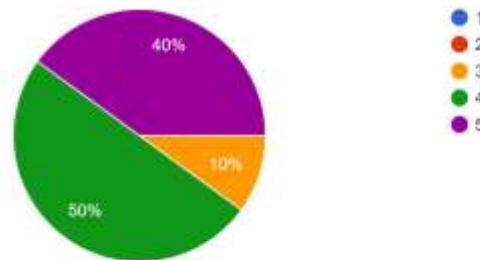


Figure 4.11: data collected from the question 4 of the questionnaire.

Do you feel an improvement moving the da Vinci arms more accurately, over the attempts?
10 respuestas

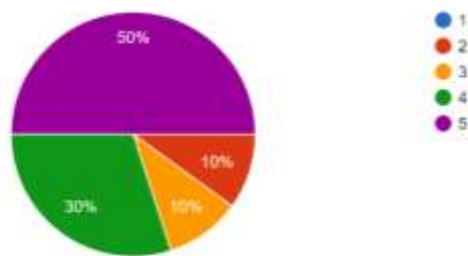


Figure 4.12: data collected from the question 5 of the questionnaire.

Do you think the visual feedback (red led light) encouraged you to be more accurate moving the PSMs?

10 respuestas

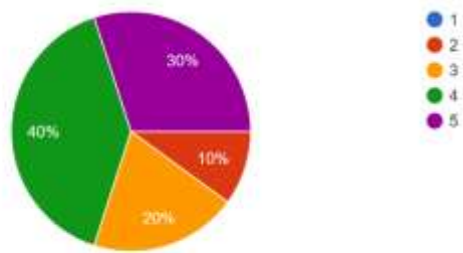


Figure 4.13: data collected from the question 6 of the questionnaire.

Chapter 5

Discussion

The results of the experimental study conducted for this thesis research indicates how assessing robotic surgical training, by means of internal and external sensors incorporated in the phantom; can be beneficial in enhancing the surgical skills and improving the learning process. The development of a realistic clinical scenario leverages the surgeon accustomed to the vision of real surgeries but also find an approach of how to control the PSMs within the body.

5.1 Benefits of implementing sensors for training assessment

Results shown in former chapter suggest that the training scenario developed, as well as the sensors implemented, benefit surgeons during the training stage; considering thus, this impact is reflexed in terms of safety and invasiveness carried into future real surgical context. Under this scope, realistic printed scenarios take a further step into training simulators by giving a visual response whenever the patient side manipulator and the organs are slightly touched, by the fact that are physical objects. Actually, since the da Vinci does not have haptic feedback, the way surgeons realise the force they are using either in clumping or pushing, is by the stretch seen on the tissue.

Furthermore, the hypothesised statement considering the impact of the sensors and assess, have been proved to be effective in this work. By considering the results shown in Tables 4.1, 4.2, 4.3, 4.4, and 4.5, it can be seen that the time request for each of the five tasks, decreases among the attempts. Therefore, this conclusion can be linked with the perceived skill improvement of the subjects, obtained from the questionnaire compiled. In this sense, providing an assessment based on objective data, can support the experienced supervisor's guidance during the evolution of the trainees.

Finally, offering a visual feedback during the training, has being probed useful, by results from the questionnaire conducted. This visual output encourages trainees to enhance the control of the master tool manipulator when sensitive organs are involved in the surgical tasks. Indeed, often, trainees, meanwhile the procedure, do not realize that the surgical arms are in contact with delicate organs, because there is no haptic feedback. Thus, this solution intends to solve this difficulty.

5.2 Limitations and Future Work

After the development of the project, one of the main drawbacks is the challenge of deciding the variables, and the lack of automation data collection. This is so, due to the fact that, taking into consideration two variables and the questionnaire for the assessment settles its methodology in variables constricted by many external factors apart from the main performance of the task. Another aspect regarding *Skill transfer*, is that the experimental protocol, consisting of three repetitions, is not enough to demonstrate that the training phase influences performance in a real surgical scenario. Finally, even though the simulated procedure has been scheduled on the basis of the FRS curriculum, either the assessment and the experimental protocol still need to be validated by a specialist surgeon.

According, therefore to future works, some steps can be done in conducting new variable measurements and sensors that are not dependent on the time, as for example, the kinematical metrics from the RAS, to introduce image processing to assess the positioning of the camera... Finally, another improvement would be to develop an experimental protocol longer in time intending to assess *Skill transfer*, and validate the variables measured and the experimental protocol.

Chapter 6

Conclusion

This work features the development of a sensorized phantom, including the segmentation of the file, the 3D characterisation of its tissue, and the experimental phase to validate the project.

The generation of the model was done by means of the segmenting program: *3D Slicer*, and an abdominal DICOM file. Followed by that, it was the 3D printing modifying each organ considering its physical properties, apart from the assembling of the organs, figure 6.1. Later on, it was studied the variables that were expected to be measured and the sensors applied to be implemented. Finally, a data collection protocol was developed to store the data from the internal and external sensors and its way to save them in an XCL file.

After the assembling of the phantom, the experimental phase conducted measured a progressive learning of the FRS tasks intended to be learnt by heart, by the trainees. Moreover, the visual feedback during the training has been probed to be an optimal way to provide a feedback to the surgeons.

Finally, as a way of achieving deeper research in this sense, it can be thought new validated metrics so measure the performance and, thus, new sensorizations. Also, it can be focused on new approaches to provide a deeper simulation environment for medium and high level trainings. Concluding, a further experimental phase based on a validated model by expert surgeons specialized on these procedures would be a pertinent research aspect.



Figure 6.1: image representatting the final printed phantom during a simulation.

Agradecimientos

I would like to thank firstly this work to Elena de Momi for giving me the chance to work in the NearLab research group and Alberto Rota for all the help offered during the development of this work, and his friendship.

Pero también debo este trabajo a mis padres y mis hermanos que me ha apoyado durante estos años en todos los sentidos. A mi gran amigo Pau por estar siempre ahí cuando lo necesitaba.. A Chimo y don Fer por guiarme en mis primeros años de carrera y ayudarme a crecer en lo personal. A Arturo y don Sebas, quienes me han hecho madurar y han sido ejemplo de trato y constancia. Y a todos mis amigos: Cabo ,Javi Casero, Camilla, David, Jaime y restodel grupo y amigos de la carrera, de los que he y contunúo aprendiendo tanto.

A tutti gli residenti dell'accademia per l'accoglienza questi ultimi mesi della mia laurea. Lorenzo Mosconi, Alessandro Rivali, Willy, Marco, Carlos, Jerry, Michelle e tanti altri..., vi tengo nel cuore.

También deo este trabajo a Hugo, Juan, Adri, Garri, Nerea, Anna, Clara y Xavi, por esos meses en Milán.

Y por último debo este trabajo a Manolo Guillén que me cuida desde arriba y enseñó a poner las últimas piedras por con quien estará disfrutado ahora.

A todos gracias,

References

- [1] Mathias Hoeckelmann, Imre J. Rudas, Paolo Fiorini, Frank Kirchner, and Tamas Haidegger. Current capabilities and development potential in surgical robotics. *International Journal of Advanced Robotic Systems*, 12, 5 2015.
- [2] Michael A. Goodrich and Alan C. Schultz. *Human-robot interaction: A survey*, 2007.
- [3] Marconi, S., Negrello, E., Mauri, V., Pugliese, L., Peri, A., Argenti, F., Auricchio, F., & Pietrabissa, A. (2019). Toward the improvement of 3D-printed vessels' anatomical models for robotic surgery training. *The International Journal of Artificial Organs*, 42(10), 558–565.
- [4] Takacs, K., Moga, K., & Haidegger, T. (2020). Sensorized Psychomotor Skill Assessment Platform Built on a Robotic Surgery Phantom. *SAMI 2020 - IEEE 18th World Symposium on Applied Machine Intelligence and Informatics, Proceedings*, 95–99. <https://doi.org/10.1109/SAMI48414.2020.9108730>
- [5] Alkatout, I., Mechler, U., Mettler, L., Pape, J., Maass, N., Biebl, M., Gitas, G., Laganà, A. S., & Freytag, D. (2021). The Development of Laparoscopy—A Historical Overview. *Frontiers in Surgery*, 8, 655. <https://doi.org/10.3389/FSURG.2021.799442/BIBTEX>
- [6] Ruurda, J. P., van Vroonhoven, T., & Broeders, I. (2002). Robot-assisted surgical systems: a new era in laparoscopic surgery. *Ann R Coll Surg Engl*, 84, 223–226.
- [7] Yingwei Guo, Yingjian Yang, Mengting Feng, Fengqiu Cao, HanhuiWu, & Yan Kang. (2020, October). Review on Development Status and Key Technologies of Surgical Robots. *International Conference on Mechatronics and Automation*. <https://ieeexplore.ieee.org/stamp/stamp.jsp?arnumber=9233776>
- [8] A. D. Alexander, “Impacts of telemation on modern society,” in *On Theory and Practice of Robots and Manipulators*, pp. 121–136, Springer, 1972.
- [9] Maier-Hein, L., Eisenmann, M., Sarikaya, D., März, K., Collins, T., Malpani, A., Fallert, J., Feussner, H., Giannarou, S., Mascagni, P., Nakawala, H., Park, A., Pugh, C., Stoyanov, D., Vedula, S. S., Cleary, K., Fichtinger, G., Forestier, G., Gibaud, B., ... Speidel, S. (2022). Surgical data science – from concepts toward clinical translation. *Medical Image Analysis*, 76. <https://doi.org/10.1016/j.media.2021.102306>
- [10] Piqué, F., Boushaki, M. N., Brancadoro, M., de Momi, E., & Menciassi, A. (2019). Dynamic Modeling of the da Vinci Research Kit Arm for the Estimation of Interaction Wrench. *2019 International Symposium on Medical Robotics, ISMR 2019*. <https://doi.org/10.1109/ISMR.2019.8710210>
- [11] Azizian, M., Liu, M., Khalaji, I., Sorger, J., Oh, D., & Daimios, S. (2020). The da Vinci Surgical System. *Handbook of Robotic and Image-Guided Surgery*, 13–27. https://doi.org/10.1007/978-3-030-17223-7_3
- [12] Bhayani, S. B. (2008). da Vinci robotic partial nephrectomy for renal cell carcinoma: an atlas of the four-arm technique. *Journal of Robotic Surgery*, 1(4), 279. <https://doi.org/10.1007/S11701-007-0055-5>
- [13] De Groote, R., Decaestecker, K., Larcher, A., Buelens, S., de Bleser, E., D’Hondt, F., Schatteman, P., Lumen, N., Montorsi, F., Mottrie, A., de Naeyer, G., de Naeyer, G., Sopena, J. M. G., Pini, G., Grivas, N., Lantz, A. W., Everaerts, W. L. M., Goonewardene,

- S., & Ploumidis, A. (2020). Robot-assisted nephroureterectomy for upper tract urothelial carcinoma: results from three high-volume robotic surgery institutions. *Journal of Robotic Surgery*, 14(1), 211–219. <https://doi.org/10.1007/S11701-019-00965-8>
- [14] Tanaka, A., Manuela Perez, M., Truong, M., Simpson Gareth Hearn, K., & Smith, R. (2014). From Design to Conception: An Assessment Device for Robotic Surgeons.
- [15] Smith, R., Patel, V., & Satava, R. (2014). Fundamentals of robotic surgery: a course of basic robotic surgery skills based upon a 14-society consensus template of outcomes measures and curriculum development. *The International Journal of Medical Robotics + Computer Assisted Surgery : MRCAS*, 10(3), 379–384. <https://doi.org/10.1002/RCS.1559>
- [16] Tanaka, A., Manuela Perez, M., Truong, M., Simpson Gareth Hearn, K., & Smith, R. (2014). From Design to Conception: An Assessment Device for Robotic Surgeons. *Interservice/Industry Training, Simulation, and Education Conference (I/ITSEC)*, 14170, 1–13.
- [17] Satava, R., Smith, R., Patel, V., Advincula, A., Aggarwal, R., Ansari, A. A., Albala, D., Angelo, R., Anvari, M., Armstrong, J., Ballantyne, G., Billia, M., Borin, J., Bouchier-Hayes, D., Brand, T., Chauhan, S., Coelho, P., Cuschieri, A., Dunkin, B., ... Weinstein, G. (2012). Fundamentals of Robotic Surgery: Outcomes Measures and Curriculum Development.
- [18] Marconi, S., Negrello, E., Mauri, V., Pugliese, L., Peri, A., Argenti, F., Auricchio, F., & Pietrabissa, A. (2019). Toward the improvement of 3D-printed vessels' anatomical models for robotic surgery training. *The International Journal of Artificial Organs*, 42(10), 558–565. <https://doi.org/10.1177/0391398819852957>
- [19] Zhu, L., Kolesov, I., Gao, Y., Kikinis, R., & Tannenbaum, A. (n.d.). An Effective Interactive Medical Image Segmentation Method Using Fast GrowCut.
- [20] Takacs, K., Moga, K., & Haidegger, T. (2020). Sensorized Psychomotor Skill Assessment Platform Built on a Robotic Surgery Phantom. *SAMI 2020 - IEEE 18th World Symposium on Applied Machine Intelligence and Informatics, Proceedings*, 95–99. <https://doi.org/10.1109/SAMI48414.2020.9108730>
- [21] Bartyzel, K. (2016). Adaptive Kuwahara filter. *Signal, Image and Video Processing*, 10(4), 663–670. <https://doi.org/10.1007/S11760-015-0791-3/FIGURES/11>
- [22] Dogra, A., & Bhalla, P. (2014). Image sharpening by Gaussian and Butterworth high pass filter. *Biomedical and Pharmacology Journal*, 7(2), 707–713. <https://doi.org/10.13005/BPJ/545>
- [23] Peter Kazanzidesf, Zihan Chen, Anton Deguet, Gregory S. Fischer, Russell H. Taylor, and Simon P. Dimaio. An open-source research kit for the da vinci® surgical system. pages 6434–6439. Institute of Electrical and Electronics Engineers Inc., 9 2014
- [24] De Groote, R., Decaestecker, K., Larcher, A., Buelens, S., de Bleser, E., D'Hondt, F., Schatteman, P., Lumen, N., Montorsi, F., Mottrie, A., de Naeyer, G., de Naeyer, G., Sopena, J. M. G., Pini, G., Grivas, N., Lantz, A. W., Everaerts, W. L. M., Goonewardene, S., & Ploumidis, A. (2020). Robot-assisted nephroureterectomy for upper tract urothelial carcinoma: results from three high-volume robotic surgery institutions. *Journal of Robotic Surgery*, 14(1), 211–219. <https://doi.org/10.1007/S11701-019-00965-8/TABLES/7>

[25] Morgan Quigley, Ken Conley, Brian Gerkey, Josh Faust, Tully Foote, Jeremy Leibs, Rob Wheeler, Andrew Y Ng, et al. Ros: an open-source robot operating system. In ICRA workshop on open source software, volume 3, page 5. Kobe, Japan, 2009